SSR Journal of Multidisciplinary (SSRJM)
Volume 3, Issue 6, 2026 Homepage: https://ssrpublisher.com/ssrjm/ ISSN: 3049-1304

Geochemical Enrichment and Surface Contamination of Heavy Metals in Soils from the Ikole–Itapaji Area, Southwestern Nigeria

Adeleke Ojo[1], Olusola Amos Olaolorun[2], and Segun Ajayi Akinyemi[3]

[1*]**ORCID:** 0009-0000-3106-2704

[1, 2 &3]Department of Geology, Faculty of Physical Sciences, Ekiti State University, Ado Ekiti

Received: *11.05.2026* | ***Accepted:*** *13.06.2026* | ***Published:*** *17.06.2026*

***Corresponding Author:** Adeleke Ojo

DOI: *10.5281/zenodo.20727669*

Abstract **Original Research Article**

Heavy metal contamination in soils poses significant environmental concerns due to its persistence and potential ecological impacts. This study assessed the distribution, mobility, enrichment, and sources of selected heavy metals (Fe, Mn, Pb, Cu, Zn, Ni, Co, Cr, and Cd) in soils from the Ikole–Itapaji area, Southwestern Nigeria. Seventeen soil samples were collected and analyzed using a modified seven-step Tessier sequential extraction procedure, Atomic Absorption Spectrophotometry (AAS), Geo-accumulation Index (Igeo), and Enrichment Factor (EF). The results show that Fe and Mn dominate all geochemical fractions, with the highest concentrations occurring in the residual phase, indicating strong lithogenic control. Most metals were concentrated in the residual, Fe–Mn oxide, and organic matter-bound fractions, while the water-soluble and exchangeable fractions contained only minor amounts, reflecting low mobility and bioavailability. Igeo and EF results indicate that Mn, Cu, Zn, Ni, Co, and Cr are mainly derived from natural weathering of the basement rocks. In contrast, Cd and Pb exhibit moderate to strong enrichment at some locations, particularly SQ3, SQ4, SQ8, and SQ15, suggesting localized anthropogenic influence. Hheavy metal distribution in the Ikole–Itapaji area is controlled predominantly by geological factors, with limited anthropogenic contributions affecting Cd and Pb. The predominance of metals in stable geochemical fractions indicates generally low environmental risk, although continued monitoring of Cd- and Pb-enriched zones is recommended.

Keywords: Heavy metals, Sequential extraction, Geo-accumulation index (Igeo), Enrichment factor (EF), Metal speciation, Soil contamination, Lithogenic source, Southwestern Nigeria.

1.0 INTRODUCTION

Heavy metals occur naturally in soils and sediments as components of parent rock materials; however, their concentrations can be significantly modified by both natural geochemical processes and anthropogenic activities. The accumulation and enrichment of trace metals in surface soils have become a major environmental concern due to their persistence, toxicity, and potential impacts on ecosystem and human health. Assessing the degree of metal enrichment and contamination is therefore essential for distinguishing natural geochemical backgrounds from human-induced inputs and for understanding the environmental implications of metal accumulation in terrestrial systems (Firmino et al., 2025).

Conventional assessments based solely on total metal concentrations provide useful information on elemental abundance but do not adequately reveal the sources, enrichment mechanisms, or environmental significance of metals within soils and sediments. Consequently, geochemical indices such as the Enrichment Factor (EF) and Geoaccumulation Index (Igeo) have been widely employed to evaluate the degree of metal contamination and to differentiate between lithogenic and anthropogenic contributions (Çelebi, 2024; Abule and Ekpete, 2025). The Enrichment Factor compares metal concentrations with a reference element and background values to determine the extent of enrichment, whereas the Geoaccumulation Index assesses contamination intensity relative to pre-industrial or background concentrations. Together, these indices provide a robust framework for evaluating metal accumulation patterns and identifying potential contamination sources in environmental studies.

In addition to pollution indices, sequential extraction techniques have become valuable tools for understanding the geochemical behavior of metals in soils and sediments. Methods such as the Tessier Sequential Extraction Procedure and the BCR Sequential Extraction Scheme partition metals into operationally defined fractions, including water-soluble, exchangeable, carbonate-bound, Fe–Mn oxide-bound, organic matter-bound, sulfide-bound, and residual phases (De Matteis et al., 2023; Ibrahim et al., 2024). These approaches provide insight into metal speciation, stability, and geochemical associations, thereby complementing contamination indices and improving interpretation of metal sources. Metals predominantly associated with residual fractions are generally considered to be of lithogenic origin and structurally bound within mineral lattices, whereas metals enriched in non-residual fractions often indicate secondary enrichment processes or anthropogenic influence (Firmino et al., 2025). Similarly, elevated concentrations within Fe–Mn oxide and organic matter fractions may reflect weathering, adsorption, and supergene enrichment processes that influence metal redistribution in soils (Delina, 2024).

The Ikole–Itapaji area of Southwestern Nigeria lies within the Precambrian Basement Complex and is underlain by migmatite–gneiss, charnockite, granitic, and related crystalline rocks that are known to influence soil geochemistry and metal distribution. Although previous studies have investigated aspects of the geology and mineralization potential of the region, information regarding the enrichment characteristics, contamination status, and source attribution of heavy metals in the soils remains limited. Understanding the extent to which metal concentrations are controlled by natural lithology or anthropogenic activities is important for both environmental assessment and mineral exploration purposes (De Matteis et al., 2023; Ibrahim et al., 2024).

Therefore, this study integrates Enrichment Factor (EF), Geoaccumulation Index (Igeo), and sequential extraction data to evaluate the enrichment patterns, contamination intensity, and geochemical sources of selected heavy metals in soils from the Ikole–Itapaji area, Southwestern Nigeria. The study aims to distinguish lithogenic and anthropogenic contributions, assess the degree of surface soil contamination, and provide insights into the geochemical processes controlling metal accumulation within this Basement Complex terrain (Firmino et al., 2025).

2.0 Description of study area

The study area is located within the Ikole–Itapaji axis of Ekiti State in Southwestern Nigeria, forming part of the Precambrian Basement Complex of the West African Craton. It lies approximately between latitudes 7°45′N–8°05′N and longitudes 5°20′E–5°40′E, covering an estimated total surface area of approximately 1,360 km². encompassing Ikole-Ekiti, Itapaji, and adjoining settlements. The terrain is characterized by undulating topography with elevations ranging from about 300 to over 600 m above sea level, typical of basement terrains marked by ridges and inselbergs (Ojo et al., 2024). Geologically, the area is dominated by migmatite–gneiss complexes, granitic intrusions, and minor schist belts, which are characteristic of the Nigerian Basement Complex and are widely associated with mineralization processes (Adetunla et al., 2025). These lithologies have

undergone multiple episodes of deformation, metamorphism, and magmatism, resulting in well-developed structural features, including faults, fractures, and joints, which serve as conduits for hydrothermal fluids (Ogah & Abubakar, 2024). The occurrence of pegmatitic intrusions within the granitic units further enhances the area's mineralization potential, particularly for rare metals.

Climatically, the region falls within the tropical humid zone, with distinct wet and dry seasons and annual rainfall exceeding 1200 mm. Vegetation is mainly derived from a savannah with patches of secondary forest, which moderately affects surface exposure during geological and remote sensing investigations. The area is relatively accessible through a network of roads linking Ikole-Ekiti to other parts of Ekiti State. Overall, the favourable lithological composition, combined with a complex structural framework, makes the Ikole–Itapaji area a promising target for integrated geophysical and remote sensing studies to delineate zones of mineralization (Salako et al., 2024).

2.1 Field description of the study area

Table 1 presents the field descriptions and geographic coordinates of seventeen (**17)** soil samples collected from different locations within the Ikole–Itapaji area of Southwestern Nigeria. The sampling points are spatially distributed across several settlements and farmland environments including Igbona-Ile, Agbeyewa Farm, Aba Farm, Esun, Omu, Iyemero, Odo-Oro, and Itapaji, thereby ensuring adequate representation of the study area. The geographic coordinates indicate that the sampled locations fall within latitudes 7°45′N to 7°59′N and longitudes 5°26′E to 5°33′E, reflecting a wide spatial coverage across the basement complex terrain. Elevation values vary considerably from 447 m to 588 m above sea level, suggesting moderate topographic variation within the study area, which may influence weathering intensity, drainage conditions, and elemental redistribution in the soils.

The sampled soils were collected at shallow depths ranging from 0.25 m to 0.60 m, representing near-surface regolith materials that are more susceptible to anthropogenic influence, weathering processes, and metal mobility. Field descriptions reveal considerable lithological and textural variability, with the soils comprising laterite, sandy clay, lateritic sand, gravelly sand, clayey sand, sandy loam, gravelly clay, and sand. Lateritic and reddish-brown soils dominate several locations such as SQ1, SQ6, SQ8, and SQ15, indicating intense tropical weathering and iron oxide enrichment typical of Precambrian Basement Complex terrains. Brown to dark brown soil colours observed in many locations suggest varying proportions of organic matter, clay minerals, and iron-bearing constituents. The occurrence of gravelly and sandy materials in some sampling points further indicates active mechanical weathering and sediment reworking processes. Overall, the field characteristics demonstrate significant heterogeneity in soil composition and morphology across the study area, which is important for understanding heavy metal distribution, geochemical partitioning, and environmental behaviour within the different sequential extraction phases.

Table 1. Field Description and Geographic Coordinates of Soil Samples Collected from the Ikole–Itapaji Area, Southwestern Nigeria

S/N	Sample ID	Locality	Latitude	Longitude	Elevation (m)	Depth (m)	Description	Colour
1	SQ1	Igbona-Ile, Ikole 1	7°45'41.9"	05°28'49.8"	564	0.35	Laterite	Reddish brown
2	SQ2	Igbona-Ile, Ikole 2	7°45'33.8"	05°26'53.6"	558	0.30	Sandy clay	Brown

S/N	Sample ID	Locality	Latitude	Longitude	Elevation (m)	Depth (m)	Description	Colour
3	SQ3	Ikole 1	7°46'23.3"	05°27'48.0"	550	0.50	Reddish brown soil	Reddish brown
4	SQ4	Agbeyewa farm	7°45'14.9"	05°28'12.6"	52	0.36	Sandy clay	Brown
5	SQ5	Ikole 2	7°50'55.8"	05°26'52.6"	556	0.40	Lateritic sand	Brown
6	SQ6	Aba farm	7°50'04.8"	05°28'16.1"	588	0.60	Laterite	Reddish brown
7	SQ7	Ikole 3	7°59'57.6"	05°27'24.0"	533	0.50	Sand	Brown
8	SQ8	Aba Dam	7°55'36.1"	05°27'42.0"	491	0.25	Laterite	Reddish brown
9	SQ9	Esun	7°45'14.9"	05°28'12.6"	541	0.28	Sandy clay	Brown
10	SQ10	Agbeyewa Farm	7°56'21.0"	05°30'20.0"	453	0.50	Gravelly sand	Grayish brown
11	SQ11	Aba Farm, Itapaji	7°58'47.0"	05°33'34.4"	447	0.34	Gravelly sand	Brown
12	SQ12	Aba Farm	7°54'23.1"	05°28'00.9"	481	0.40	Clayey sand	Brown
13	SQ13	Omu	7°53'18.9"	05°27'42.3"	503	0.30	Sand	Brown
14	SQ14	Itapaji	7°52'49.9"	05°31'05.2"	501	0.35	Sandy loam	Dark brown
15	SQ15	Iyemero	7°45'52.6"	05°33'06.3"	586	0.30	Laterite	Reddish brown
16	SQ16	Odo- Oro	7°49'45.0"	05°31'39.9"	578	0.35	Gravelly clay	Brown
17	SQ17	Ikole 4	7°50'46.3"	05°33'20.5"	543	0.40	Gravelly sand	Brown

2.2 Regional Geological Setting

The study area is located within southwestern Nigeria, forming part of the Precambrian Basement Complex of the West African Craton. This crystalline basement terrain is distinct from the surrounding sedimentary basins, including the Sokoto Basin, Chad Basin, Bida Basin, and the Benue Trough, which are largely composed of Cretaceous to Tertiary sediments (Ojo et al., 2024). The southwestern region, including the Ikole–Itapaji axis, is dominated by crystalline rocks that have undergone extensive tectono-metamorphic evolution. The Nigerian Basement Complex evolved through multiple orogenic events, notably the Liberian, Eburnean, and Pan-African cycles, which resulted in widespread deformation, metamorphism, and granitoid emplacement (Adetunla et al., 2025). These processes led to the development of major lithological units, including the migmatite–gneiss complex, schist belts, and Pan-African granitoids. In the study area, migmatite–gneiss and granitic rocks are predominant, with minor metasedimentary occurrences.

Structurally, the area is characterized by well-developed faults, fractures, and foliations, predominantly trending NE–SW and NW–SE, reflecting the imprint of the Pan-African deformational event (Ogah & Abubakar, 2024). These structures are critical in controlling hydrothermal fluid flow and mineral deposition. Mineralization within the Basement Complex is commonly associated with quartz veins, pegmatites, and shear zones. The presence of granitic and pegmatitic intrusions within the Ikole–Itapaji area further suggests favourable conditions for mineralization. Recent studies have demonstrated the effectiveness of integrated

geophysical methods in delineating such structurally controlled mineralized zones (Salako et al., 2024). The geological framework of the study area reflects a complex interplay of lithology and structure, providing a suitable environment for mineralization and justification for integrated geophysical and remote sensing investigations **(Fig. 1)**

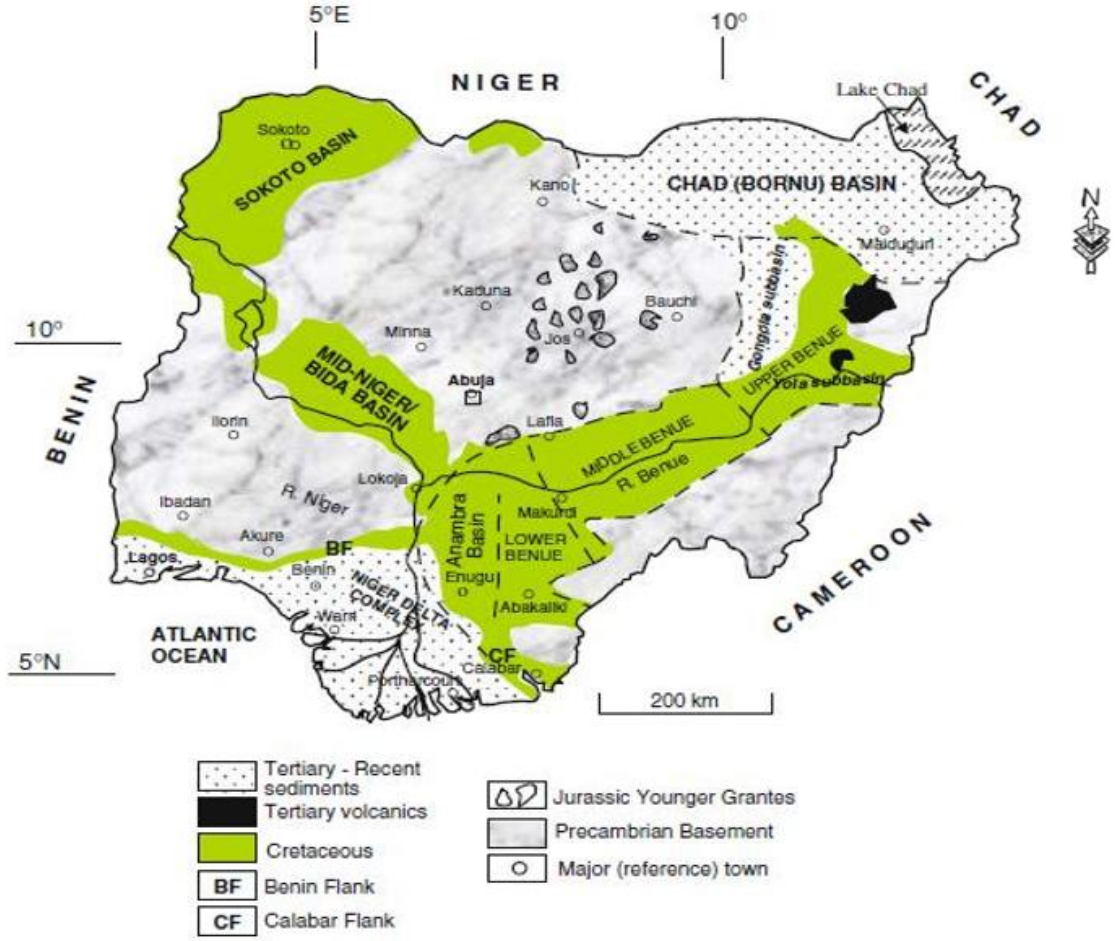

Figure 1: Geological map of Nigeria showing the distribution of major lithological units, including the Precambrian Basement Complex and surrounding sedimentary basins (Sokoto, Chad, Bida, and Benue Trough). The study area (Ikole–Itapaji, southwestern Nigeria) is located within the Basement Complex.

2.3 Geologic Map of the Study Area

The geological map of the study area reveals the major lithological units within the Precambrian Basement Complex of Southwestern Nigeria, particularly within the Ekiti basement terrain. The area has experienced complex tectonic, metamorphic, and magmatic activities associated mainly with the Pan-African orogeny (~600 ± 150 Ma) (Rahaman, 1988; Oyinloye, 2011). The dominant rock units include migmatite, granite gneiss, charnockite, and granodiorite.

Migmatite (Mg) occurs mainly in the southern and central portions around Ikole and Odo Oro. These rocks represent some of the oldest basement units and were formed through partial melting under high-grade metamorphic

conditions. Granite gneiss (GG) is the most extensive lithology, occupying the northern, central, and western parts of the area, including Itapaji and Bolorunduro. These foliated granitic rocks are structurally competent and commonly host deformation features such as fractures and faults (Oyinloye, 2011).

Charnockite (Ch) occurs locally along the western margin of the study area and represents high-temperature granulite-facies rocks associated with deep crustal processes (Rahaman, 1988). Granodiorite (OGd) forms a major intrusive body within the north-central part of the area and belongs to the Older Granite suite emplaced during the late stages of the Pan-African orogeny. These intrusions commonly occupy structurally weak zones within the basement complex (Oyinloye, 2011) (**Fig. 2**).

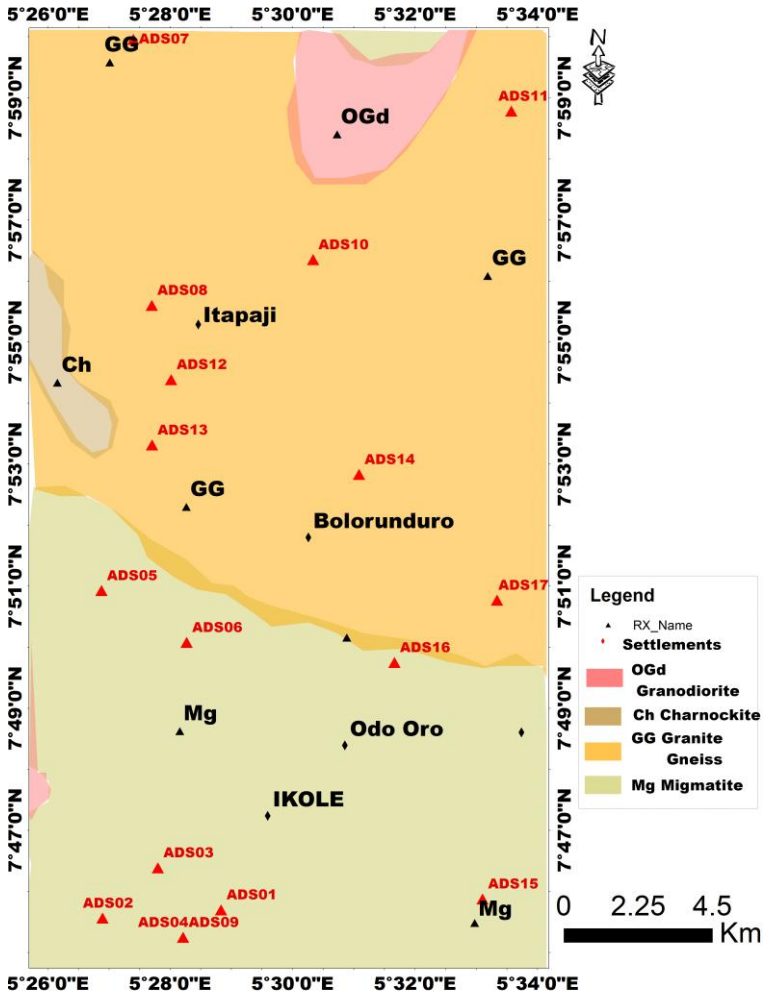

Figure 2: **Geological map of the study area after NGSA (2006). The map delineates the distribution of major lithological units and their spatial relationships. It provides a foundational framework for structural interpretation and mineral exploration within the study area.**

2.4 Sampling points from the study area

Figure 3 illustrates the spatial distribution of the seventeen soil sampling locations (SQ1–SQ17) within the Ikole–Itapaji area of Southwestern Nigeria. The study area covers approximately 16 km in the north–south direction and about 8 km east–west and forms part of the Precambrian

Basement Complex of Nigeria, which has undergone extensive tectonic, metamorphic, and magmatic evolution associated with the Pan-African orogeny (Rahaman, 1988; Oyinloye, 2011). The mapped area encompasses major settlements including Ikole, Itapaji, Odo-Oro, Bolorunduro, and adjoining rural communities where systematic soil sampling was undertaken.

The sampling locations were strategically distributed across the study area to achieve adequate spatial representation of the different topographic, and land-use settings. The distribution pattern does not follow a rigid grid system but rather a purposive sampling approach designed to capture variations in parent rock composition, weathering intensity, drainage influence, and anthropogenic activities. A relatively higher density of sampling points occurs around the Ikole–Itapaji axis, reflecting the geological significance, accessibility, and land-use intensity of these areas (Oyinloye, 2011).

Furthermore, some sampling points were positioned close to drainage channels and low-lying areas to assess the effects of surface runoff, leaching, sediment transport, and elemental redistribution on soil geochemistry.

The topographic map underlying Figure 3 reveals moderate relief characterized by ridges, slopes, and valley systems typical of Basement Complex terrains. Sampling locations are distributed across different geomorphological settings, including uplands, midslopes, and valley bottoms, thereby ensuring that the influence of topography on weathering intensity, soil development, and trace metal accumulation is adequately represented. In addition, the proximity of several sampling points to settlements and cultivated lands provides an opportunity to evaluate the potential contribution of anthropogenic activities, including agriculture and land-use practices, to heavy metal enrichment (Oyinloye, 2011.

Overall, the integration of topographic information, drainage characteristics, and systematic soil sampling provides a robust basis for understanding the relationships among geomorphological processes, weathering, and heavy metal distribution within the Ikole–Itapaji area.

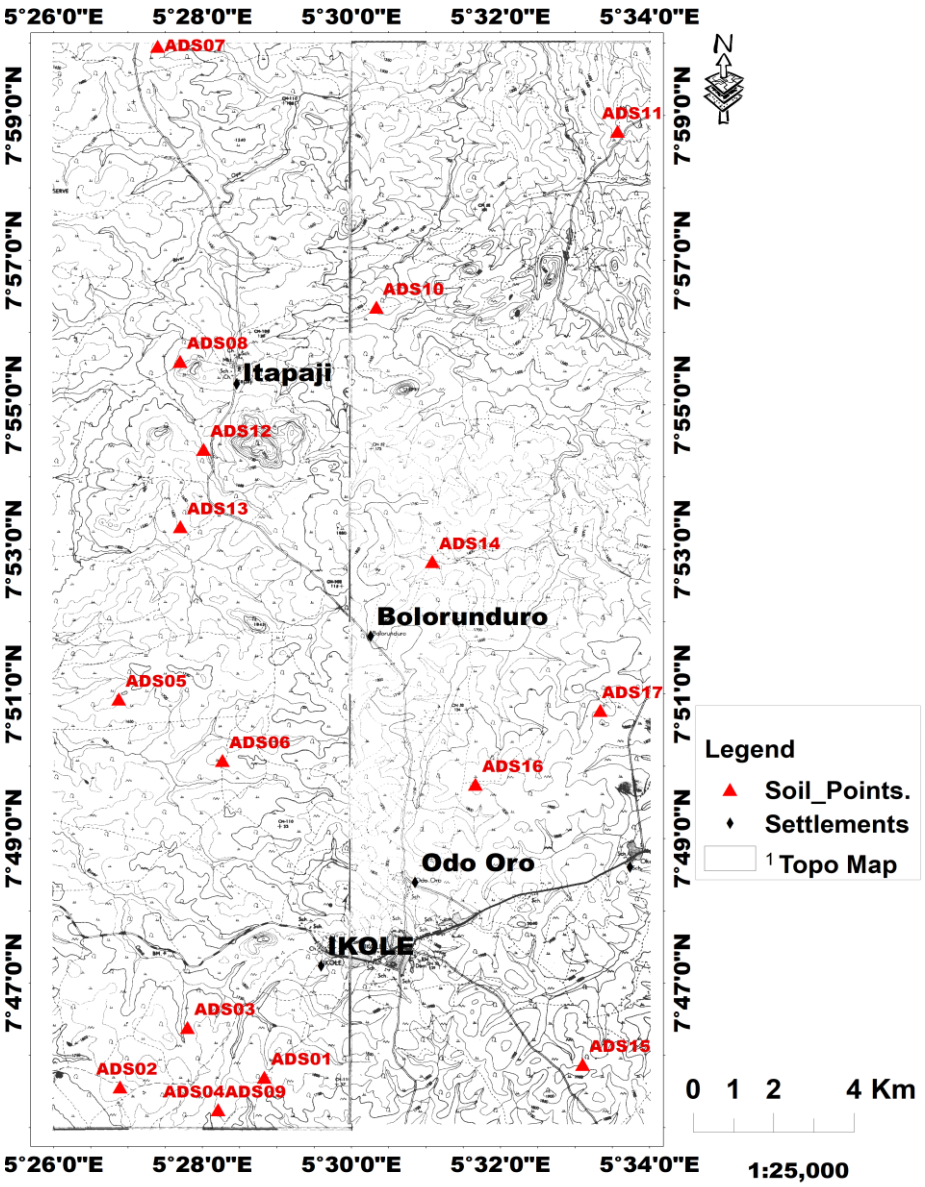

Figure 3. Topographic map of the study area showing the locations of sampled points used for geological, geochemical, and petrographic investigations.

3. 0 Materials and Methods

3.1 Sample Collection and Preparation

Soil/sediment samples were collected from selected locations within Ikole-Itapaji. The samples were obtained at shallow depths to represent the surficial geochemical environment of the study area. Each sample was air-dried at room temperature, gently disaggregated, and sieved to obtain the <63 µm fraction, which is known to retain higher concentrations of trace metals due to its large surface area and adsorption capacity.

A representative mass of 1.0 g of each prepared sample was weighed into clean centrifuge tubes for sequential extraction analysis.

3.2 Sequential Extraction Procedure

A seven-step sequential extraction procedure, modified from the widely adopted Tessier extraction scheme, was employed to partition metals into operationally defined geochemical fractions. This approach enables the differentiation of metals based on their binding strength and geochemical associations within

sediments and soils. The procedure was designed to extract metals associated with water-soluble, exchangeable, carbonate-bound, Fe–Mn oxide-bound, organic-bound, sulfide/strongly bound, and residual phases.

Sequential extraction techniques have been widely applied in recent studies to evaluate the mobility, bioavailability, and environmental risk of trace metals in soils and sediments, as they provide more reliable information than total metal concentrations alone (De Matteis et al., 2023; Bouazizi et al., 2023). The method operates on the principle of selective dissolution, where specific reagents target distinct mineralogical or geochemical phases, allowing for detailed characterization of metal partitioning (Doi et al., 2023;). Recent modifications of the classical Tessier procedure have demonstrated improved efficiency, reproducibility, and applicability across diverse environmental matrices, including contaminated sediments and mining-impacted soils (Çelebi, 2024; Souza et al., 2024).

The adopted seven-step scheme provides enhanced resolution of metal speciation, particularly in distinguishing weakly bound fractions from those strongly incorporated within mineral lattices, thereby offering critical insights into both environmental behavior and mineralization processes.

The extraction steps were carried out as follows:

Phase 1: Water-Soluble Fraction

Twenty milliliters (20 mL) of deionized water was added to 1.0 g of sample and agitated for 1 hour at room temperature. The mixture was centrifuged, and the supernatant was decanted for analysis.

Phase 2: Exchangeable Fraction

Twenty milliliters (20 mL) of 1 M $MgCl_2$ solution was added to the residue from Phase 1 and shaken for 1 hour. The mixture was centrifuged, and the extract was collected.

Phase 3: Carbonate-Bound Fraction

Twenty milliliters (20 mL) of 1 M sodium acetate (NaOAc) adjusted to pH 5 was added to the residue from Phase 2 and shaken for 5 hours. After centrifugation, the extract was filtered and preserved.

Phase 4: Fe–Mn Oxide (Reducible) Fraction

Twenty milliliters (20 mL) of hydroxylamine hydrochloride ($NH_2OH \cdot HCl$) solution was added to the residue from Phase 3 and heated at approximately 95°C for 2 hours with intermittent agitation. The mixture was cooled, centrifuged, and the extract was collected.

Phase 5: Organic Matter-Bound Fraction

Ten milliliters (10 mL) of acidified hydrogen peroxide (H_2O_2) was added to the residue from Phase 4 and heated at 85°C for 2 hours. A second aliquot of 10 mL H_2O_2 was added, followed by repeated heating. After cooling, 20 mL of ammonium acetate (NH_4OAc) was added, and the mixture was shaken for 30 minutes before centrifugation and collection of the extract.

Phase 6: Sulfide/Strongly Bound Fraction

Fifteen milliliters (15 mL) of concentrated nitric acid (HNO_3) was added to the residue from Phase 5 and heated gently to near dryness. The residue was cooled, diluted, centrifuged, and the extract was collected.

Phase 7: Residual Fraction

The final residue was digested using a mixture of hydrofluoric acid (HF), perchloric acid ($HClO_4$), and nitric acid (HNO_3) until complete dissolution was achieved. The digest was appropriately diluted for analysis.

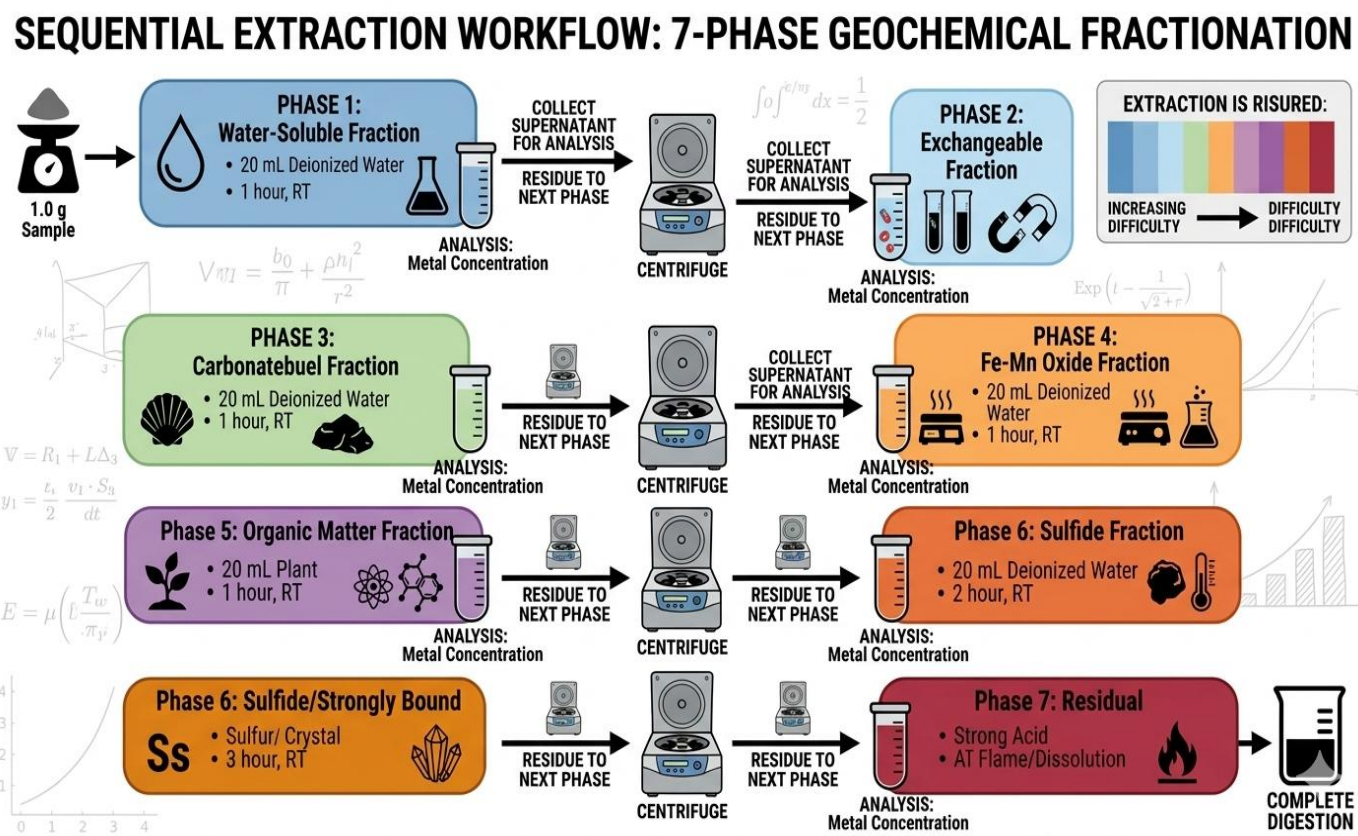

3.3 Geochemical Pollution Indices

Trace metal concentrations were determined using **Atomic Absorption Spectrophotometry (AAS)** (Buck Scientific Model 205A) with an air–acetylene flame. Calibration standards were prepared using appropriate matrix-matched solutions to ensure analytical accuracy.

For each fraction, the supernatant was diluted where necessary (typically 20–50×), and concentrations were obtained from calibration curves. All analyses were conducted in triplicate, and reagent blanks were included to ensure quality control.

For total metal determination (residual fraction), samples were subjected to strong acid digestion using HF–$HClO_4$–HNO_3 mixtures to ensure complete dissolution of silicate matrices, following standard geochemical digestion protocols.

3.3.1 Enrichment Factor (EF)

The **Enrichment Factor (EF)** was used to assess the degree of anthropogenic influence and contamination in the study area. It was calculated as:

$$EF = (Cn / Cref)sample / (Bn / Bref)\ background \quad (1)$$

where:

Cn = concentration of target metal in sample,

C_{ref} = concentration of reference element (commonly Fe or Al),

Bn and B_{ref} = background concentrations.

The EF classification is as follows:

- EF < 2: Deficiency to minimal enrichment
- 2 ≤ EF < 5: Moderate enrichment
- 5 ≤ EF < 20: Significant enrichment

20 ≤ EF < 40: Very high enrichment

EF ≥ 40: Extremely high enrichment

3.3.2 Geo-accumulation Index (Igeo)

The Geoaccumulation Index (Igeo) was used to

assess the degree of metal pollution by comparing current concentrations with pre-industrial background values. It was calculated using the relationship:

$$Igeo = log2\,(Cn / (1.5 \times Bn)) \quad (2)$$

where:
Cn represents the measured concentration of a metal in the sample,
Bn represents the geochemical background concentration (average shale value),
1.5 is the correction factor for natural lithological variations.

Igeo values classify sediments from unpolluted to extremely polluted depending on the degree of enrichment relative to natural background.

Table 2. Average shale values of selected heavy metals used as geochemical background concentrations for pollution assessment in the study area (Turekian and Wedepohl, 1961).

S/N	Metal	Shale Value (mg/kg)
1	Fe	47,200
2	Mn	850
3	Pb	20
4	Cu	45
5	Zn	95
6	Ni	68
7	Co	19
8	Cr	90
9	Cd	0.3

4.0 Results and discussion

4.1 Water-soluble phase

The water-soluble phase represents the most mobile and bioavailable fraction of metals in soils and sediments, and it is typically very low in natural systems due to strong mineral binding (Kabata-Pendias, 2011; Alloway, 2013).

Results in **Table 3a** show generally low concentrations of all metals across samples (SQ1–SQ17), indicating limited dissolution into pore water. Fe records the highest values (2.873–7.427 mg/kg), reflecting relatively higher geochemical reactivity but still low mobility due to strong association with silicate and oxide minerals. Mn ranges from 1.742–3.128 mg/kg, showing slight variation linked to redox sensitivity (Reimann & de Caritat, 2012). Cu (0.163–0.742 mg/kg) and Zn (0.126–0.627 mg/kg) are low, suggesting natural weathering control, while Pb (0.049–0.098 mg/kg) and Cd (0.002–0.007 mg/kg) indicate minimal contamination and strong retention in solid phases. Ni, Co, and Cr also remain consistently low across samples.

The statistical summary in **Table 3b** confirms low variability, with mean concentrations ordered as Fe > Mn > Cu ≈ Zn > Pb > Co ≈ Ni > Cr > Cd. This indicates dominance of lithogenic control with very limited metal mobility. The spatial distribution shown in **Figure 4** (cluster column chart**)** supports these observations,

clearly illustrating the dominance of Fe and Mn across all samples. At the same time, other metals remain uniformly low with no distinct spatial anomaly. The clustering pattern confirms that variations are minor and do not reflect pollution hotspots but natural geochemical background levels (Hakanson, (1980).

Overall, the combined interpretation of **Table 3a, Table 3b, and Figure 4** indicates low mobility, weak aqueous dispersion, and strong lithogenic control of metals in the water-soluble phase, with negligible environmental risk under current conditions.

Table 3a. Heavy metals concentration in the water-soluble phase (mg/kg) of sediments/soils from the Ikole–Itapaji area, Southwestern Nigeria. This fraction represents the most mobile and immediately bioavailable portion of trace metals, reflecting their potential short-term environmental availability and mobility in the near-surface environment.

Samples	Fe (mg/Kg)	Mn (mg/Kg)	Pb (mg/Kg)	Cu (mg/Kg)	Zn (mg/Kg)	Ni (mg/Kg)	Co (mg/Kg)	Cr (mg/Kg)	Cd (mg/Kg)
SQ 1	6.321	2.087	0.077	0.681	0.572	0.054	0.062	0.023	0.004
SQ 2	6.128	2.063	0.072	0.631	0.509	0.059	0.063	0.021	0.003
SQ 3	7.427	3.108	0.083	0.724	0.592	0.063	0.069	0.028	0.005
SQ 4	7.129	3.099	0.081	0.711	0.579	0.061	0.066	0.025	0.005
SQ 6	5.873	2.145	0.094	0.742	0.582	0.063	0.067	0.029	0.006
SQ7	4.568	1.958	0.064	0.465	0.368	0.043	0.048	0.016	0.003
SQ 8	6.409	2.056	0.076	0.641	0.539	0.052	0.063	0.022	0.004
SQ 10	2.873	1.742	0.049	0.163	0.126	0.034	0.037	0.013	0.002
SQ 11	3.208	1.839	0.056	0.218	0.189	0.041	0.045	0.015	0.003
SQ 12	5.175	2.094	0.086	0.598	0.565	0.061	0.057	0.024	0.005
SQ 13	5.387	2.109	0.087	0.605	0.591	0.063	0.054	0.026	0.005
SQ 14	6.125	2.135	0.092	0.676	0.608	0.067	0.061	0.029	0.006
SQ 15	7.105	3.128	0.091	0.624	0.573	0.056	0.054	0.031	0.006
SQ 16	5.891	2.207	0.095	0.673	0.606	0.065	0.059	0.034	0.007
SQ 17	5.006	1.876	0.098	0.659	0.627	0.064	0.062	0.033	0.007

Table 3b. Statistical summary of the heavy metals concentration in the water-soluble phase (mg/kg). This table presents the minimum, maximum, and mean concentrations of the selected metals across all samples in the study area. It provides a simplified statistical overview of metal distribution and mobility within the most labile geochemical fraction of the soil–sediment system.

Metal	Fe	Mn	Pb	Cu	Zn	Ni	Co	Cr	Cd
Min	2.873	1.742	0.049	0.163	0.126	0.034	0.037	0.013	0.002
Max	7.427	3.128	0.098	0.742	0.627	0.067	0.069	0.034	0.007
Mean	5.642	2.243	0.080	0.587	0.508	0.056	0.058	0.025	0.005

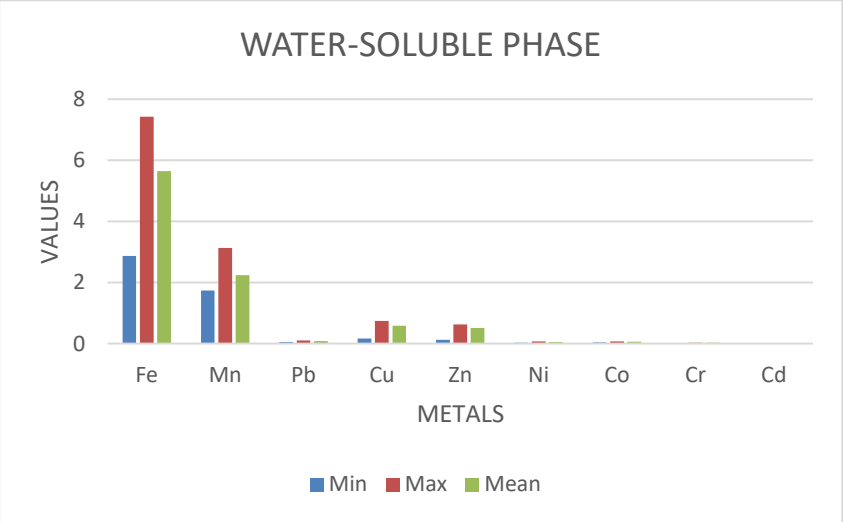

Figure 4. Cluster column chart of heavy metal concentrations in the water-soluble phase (mg/kg). The figure illustrates the comparative distribution of selected metals across all samples, highlighting variations in their mobility and relative abundance within the most labile geochemical fraction.

4.2 The exchangeable phase

The exchangeable phase consists of metals weakly adsorbed to soil surfaces and is environmentally important because such metals can be released under changes in pH, ionic strength, or competing ions (Kabata-Pendias, 2011; Alloway, 2013).

Table 4a shows higher metal concentrations than the water-soluble phase, indicating stronger but reversible adsorption to soil exchange sites. Fe is dominant (5.731–10.742 mg/kg), reflecting strong association with clay and oxide minerals. Mn (1.342–3.127 mg/kg) shows moderate variability linked to redox sensitivity (Alloway, 2013).

Cu (0.279–0.967 mg/kg) and Zn (0.261–0.886 mg/kg) are moderately retained, while Pb (0.082–0.146 mg/kg) and Cd (0.004–0.029 mg/kg) remain low but slightly enriched, indicating potential mobility under acidic conditions. Ni, Co, and Cr are consistently low, reflecting partial release from primary minerals. **Table 4b** shows the mean order: **Fe > Mn > Cu > Zn > Pb > Ni > Co > Cr > Cd**, confirming Fe and Mn dominance (Hakanson, (1980).

Spatially, SQ3, SQ4, SQ14, SQ15, and SQ17 show higher values, while SQ10 is the lowest, suggesting natural lithological control rather than contamination. This pattern is supported by

Figure 5, which highlights clear Fe–Mn dominance, moderate Cu–Zn clustering, and uniformly low Pb, Cd, Ni, Co, and Cr across samples.

Overall, the exchangeable phase exhibits moderate metal retention and limited mobility, controlled primarily by clay minerals and organic matter. The presence of Pb and Cd, though low, indicates potential sensitivity to environmental changes such as acidification (Kabata-Pendias, 2011; Alloway, 2013).

Table 4a: Exchangeable phase of the heavy metal concentrations in soil samples (mg/kg). The table presents the distribution of Fe, Mn, Pb, Cu, Zn, Ni, Co, Cr, and Cd across all sampling locations, reflecting metals weakly bound to soil exchange sites and their potential environmental mobility.

Samples	Fe (mg/Kg)	Mn (mg/Kg)	Pb (mg/Kg)	Cu (mg/Kg)	Zn **(mg/Kg)**	Ni (mg/Kg)	Co (mg/Kg)	Cr (mg/Kg)	Cd (mg/Kg)
SQ 1	8.084	1.875	0.098	0.789	0.701	0.072	0.071	0.031	0.007
SQ 2	8.005	1.802	0.097	0.712	0.685	0.073	0.069	0.032	0.005
SQ 3	10.742	2.085	0.102	0.826	0.732	0.081	0.075	0.037	0.029
SQ 4	10.488	2.016	0.108	0.813	0.735	0.085	0.076	0.037	0.028
SQ 6	6.402	2.073	0.112	0.839	0.784	0.082	0.073	0.042	0.009
SQ7	6.023	1.762	0.082	0.619	0.586	0.065	0.059	0.025	0.005
SQ 8	8.787	1.904	0.126	0.804	0.721	0.075	0.073	0.034	0.026
SQ 10	5.731	1.342	0.085	0.279	0.261	0.067	0.072	0.026	0.004
SQ 11	6.174	1.563	0.096	0.351	0.31	0.071	0.072	0.029	0.005
SQ 12	7.787	2.012	0.113	0.801	0.721	0.094	0.087	0.038	0.009
SQ 13	7.819	2.105	0.109	0.799	0.726	0.097	0.085	0.042	0.01
SQ 14	8.534	3.083	0.138	0.902	0.846	0.102	0.095	0.051	0.017
SQ 15	10.231	3.127	0.146	0.927	0.872	0.117	0.102	0.054	0.021
SQ 16	7.118	2.105	0.128	0.942	0.839	0.112	0.11	0.059	0.028
SQ 17	6.104	2.098	0.131	0.967	0.886	0.132	0.121	0.061	0.026

Table 4b: Statistical summary of the heavy metals concentration in the exchangeable phase (mg/kg). This table presents the minimum, maximum, and mean concentrations of selected metals across all samples in the exchangeable fraction. It highlights the variability and relative mobility of metals weakly bound to soil exchange sites, which are potentially available for environmental release.

Metal	Fe	Mn	Pb	Cu	Zn	Ni	Co	Cr	Cd
Min	5.731	1.342	0.082	0.279	0.261	0.065	0.059	0.025	0.004
Max	10.742	3.127	0.146	0.967	0.886	0.132	0.121	0.061	0.029
Mean	7.869	2.064	0.111	0.758	0.694	0.088	0.083	0.040	0.015

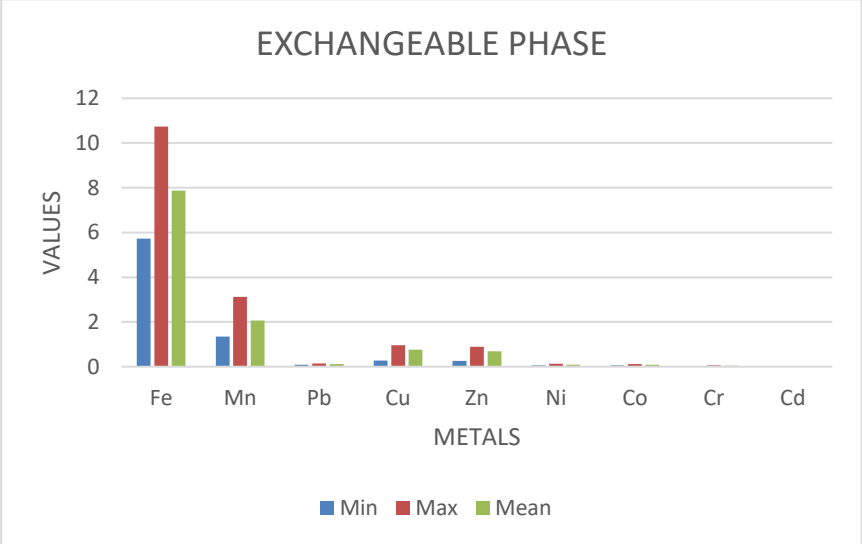

Figure 5. Cluster column chart of heavy metal concentrations in the exchangeable phase (mg/kg). The figure illustrates the comparative distribution of metals across all samples in the exchangeable fraction, highlighting variations in their relative mobility and binding strength to soil exchange sites.

4.3 The carbonate-bound phase

The carbonate-bound phase comprises metals associated with carbonate minerals and is sensitive to pH changes, particularly under acidic conditions where dissolution can release bound metals (Kabata-Pendias, 2011; Alloway, 2013).

Table 5a shows a clear increase in metal concentrations compared to earlier fractions, indicating stronger incorporation into carbonate phases. Fe (36.325–66.488 mg/kg) and Mn (23.728–38.019 mg/kg) dominate, reflecting their affinity for co-precipitation with carbonates. Zn (12.101–19.807 mg/kg) and Cu (1.112–3.213 mg/kg) show moderate enrichment, while Pb (1.025–3.832 mg/kg) indicates stable carbonate association. Ni, Co, and Cr occur at lower but consistent levels, and Cd remains low (0.054–0.121 mg/kg). The statistical summary in **Table 5b** confirms the trend: Fe > Mn > Zn > Pb > Cu > Ni > Co > Cr > Cd (Hakanson, (1980)

Spatially, higher values in SQ3, SQ4, and SQ15 contrast with lower concentrations in SQ10, reflecting lithological variability rather than contamination. This pattern is supported by **Figure 6**, which highlights Fe–Mn dominance, moderate Zn–Cu enrichment, and consistently lower levels of other metals across samples. Overall, the carbonate-bound phase represents a moderately stable metal reservoir with potential mobility under acidic conditions, although current distributions indicate strong lithogenic control.

Table 5a. Heavy metal concentrations in the carbonate-bound phase (mg/kg). The table shows the distribution of metals associated with carbonate minerals across all samples, reflecting their relative stability and potential release under acidic environmental conditions.

Samples	Fe (mg/Kg)	Mn (mg/Kg)	Pb (mg/Kg)	Cu (mg/Kg)	Zn (mg/Kg)	Ni (mg/Kg)	Co (mg/Kg)	Cr (mg/Kg)	Cd (mg/Kg)
SQ 1	40.129	25.207	2.279	2.439	13.226	2.147	1.701	0.531	0.069
SQ 2	41.052	25.422	2.142	2.197	13.055	2.132	1.626	0.625	0.065
SQ 3	65.246	37.529	3.217	2.826	18.614	2.704	2.002	0.954	0.089
SQ 4	66.488	38.019	3.832	3.213	18.901	3.125	2.106	1.005	0.103
SQ 6	38.615	24.234	1.715	2.327	13.178	2.362	1.448	0.603	0.059
SQ7	38.247	24.127	1.665	2.401	13.218	2.295	1.353	0.616	0.055
SQ 8	41.271	25.431	3.102	2.424	13.286	2.149	1.747	1.103	0.072
SQ 10	36.325	23.728	1.025	1.112	12.521	1.891	0.829	0.518	0.054
SQ 11	37.623	24.061	2.611	2.103	12.101	2.047	1.521	0.556	0.055
SQ 12	39.114	25.716	3.112	2.518	12.224	2.104	1.687	0.738	0.069
SQ 13	38.864	24.612	3.109	2.429	12.138	2.049	1.716	0.742	0.071
SQ 14	41.451	26.128	2.234	2.657	13.441	2.162	1.392	0.671	0.077
SQ 15	46.539	37.423	3.627	2.985	19.807	3.127	2.108	1.054	0.121
SQ 16	41.318	25.035	2.512	2.548	13.033	2.102	1.711	1.005	0.098
SQ 17	38.712	24.291	2.271	2.462	12.987	1.937	1.491	0.657	0.097

Table 5b. Statistical summary of the heavy metals in the carbonate-bound phase (mg/kg). The table presents the minimum, maximum, and mean concentrations of metals associated with carbonate fractions, highlighting their relative enrichment and stability within this geochemical phase.

Metal	Fe	Mn	Pb	Cu	Zn	Ni	Co	Cr	Cd
Min	36.325	23.728	1.025	1.112	12.101	1.891	0.829	0.518	0.054
Max	66.488	38.019	3.832	3.213	19.807	3.127	2.108	1.103	0.121
Mean	43.580	26.998	2.630	2.450	13.915	2.235	1.629	0.758	0.078

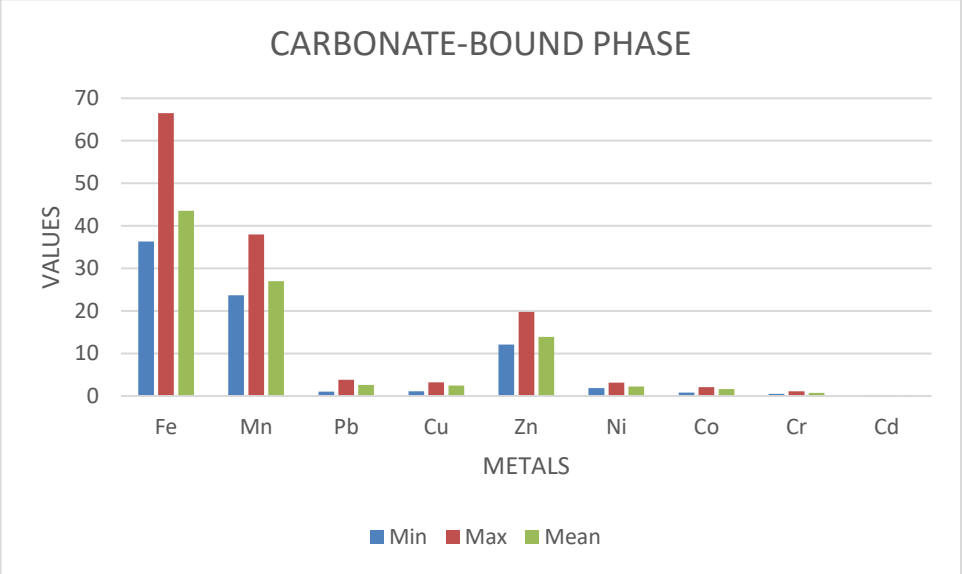

Figure 6. Cluster column chart of the heavy metal concentrations in the carbonate-bound phase (mg/kg). The figure illustrates the comparative distribution of metals across all samples, highlighting their relative enrichment and association with carbonate minerals within this geochemical fraction.

4.4 The Fe–Mn oxide phase

Table 6a and 6b present the distribution and statistical summary of heavy metals associated with the Fe–Mn oxide fraction across the studied soil samples. This geochemical phase is particularly important because iron and manganese oxides are known to have strong adsorption capacities and therefore act as major sinks for trace metals in soil environments (Kabata-Pendias, 2011; Alloway, 2013). The results show that Fe and Mn occur in relatively high concentrations across all samples, with Fe ranging from 303.187 to 476.031 mg/kg and Mn from 139.204 to 267.163 mg/kg. These elevated values reflect the dominance of Fe–Mn oxides in controlling metal retention and indicate strong scavenging of trace elements during secondary soil-forming processes.

Among the trace metals, Zn shows comparatively higher concentrations (54.584–77.129 mg/kg), followed by Pb (16.623–36.125 mg/kg), Cu (11.197–22.957 mg/kg), and Ni (16.352–26.103 mg/kg). Co, Cr, and Cd occur at lower but still significant levels, indicating variable affinity for Fe–Mn oxide surfaces. The highest metal loadings are observed in samples SQ3, SQ4, and SQ15, suggesting localized enrichment possibly linked to lithological variation or enhanced adsorption under specific geochemical conditions Wei & Yang, (2010). In contrast, samples such as SQ10 consistently record the lowest concentrations, indicating weaker metal retention capacity in those locations.

The statistical summary (Table 4b) further confirms the strong geochemical association of metals with Fe–Mn oxides, with mean concentrations following the order Fe > Mn > Zn > Pb > Cu > Ni > Co > Cr > Cd. The relatively high mean values of Zn, Pb, and Cu suggest significant anthropogenic influence superimposed on natural geochemical processes. Overall, the Fe–Mn oxide fraction plays a critical role in controlling metal mobility and redistribution in the study area, as these oxides can effectively adsorb and immobilize trace metals under varying redox conditions (Tessier et al., 1979; Wei & Yang, 2010).

Table 6a: Heavy metal concentrations in the Fe–Mn oxide phase (mg/kg). The table presents the distribution of metals associated with iron and manganese oxides across all samples, reflecting their strong adsorption capacity and role as key geochemical sinks for trace elements.

Samples	Fe (mg/Kg)	Mn (mg/Kg)	Pb (mg/Kg)	Cu (mg/Kg)	Zn **(mg/Kg)**	Ni (mg/Kg)	Co (mg/Kg)	Cr (mg/Kg)	Cd (mg/Kg)
SQ 1	354.813	152.227	25.711	13.403	63.866	19.181	10.271	6.361	0.621
SQ 2	361.558	175.129	22.019	15.019	63.545	20.196	11.287	6.185	0.657
SQ 3	435.209	237.214	33.277	20.236	74.091	22.573	14.263	9.159	1.872
SQ 4	446.513	241.116	35.332	21.873	77.129	26.103	14.742	10.015	1.983
SQ 6	362.145	154.434	26.072	12.615	63.071	20.032	10.481	5.235	0.598
SQ7	358.903	149.828	21.612	13.211	63.242	18.269	9.593	6.062	0.615
SQ 8	371.874	185.401	26.128	14.029	70.008	20.542	11.792	8.187	1.328
SQ 10	303.187	139.204	16.623	11.197	54.584	16.352	6.282	4.815	0.574
SQ 11	337.217	144.436	18.217	12.018	58.611	19.142	8.027	5.251	0.591
SQ 12	349.812	147.164	23.712	16.182	62.202	20.017	10.019	6.131	0.691
SQ 13	345.875	147.119	23.389	16.429	62.138	20.049	9.948	5.782	0.711
SQ 14	360.158	176.524	25.304	15.173	63.493	21.366	11.097	7.176	0.877
SQ 15	476.031	267.163	36.125	22.957	75.937	25.183	13.162	10.254	2.021
SQ 16	361.521	155.003	22.574	14.348	64.113	19.179	11.201	7.012	0.798
SQ 17	338.019	142.401	17.753	12.967	59.285	18.331	10.096	8.954	0.917

Table 6b: Statistical summary of the heavy metals concentration in the Fe–Mn oxide phase (mg/kg). The table shows the minimum, maximum, and mean concentrations of metals bound to Fe–Mn oxides, highlighting their significant enrichment and strong affinity for adsorption within this geochemical fraction.

Metal	Fe	Mn	Pb	Cu	Zn	Ni	Co	Cr	Cd
Min	303.187	139.204	16.623	11.197	54.584	16.352	6.282	4.815	0.574
Max	476.031	267.163	36.125	22.957	77.129	26.103	14.742	10.254	2.021
Mean	370.456	173.958	24.790	15.977	65.554	20.454	10.751	7.122	0.923

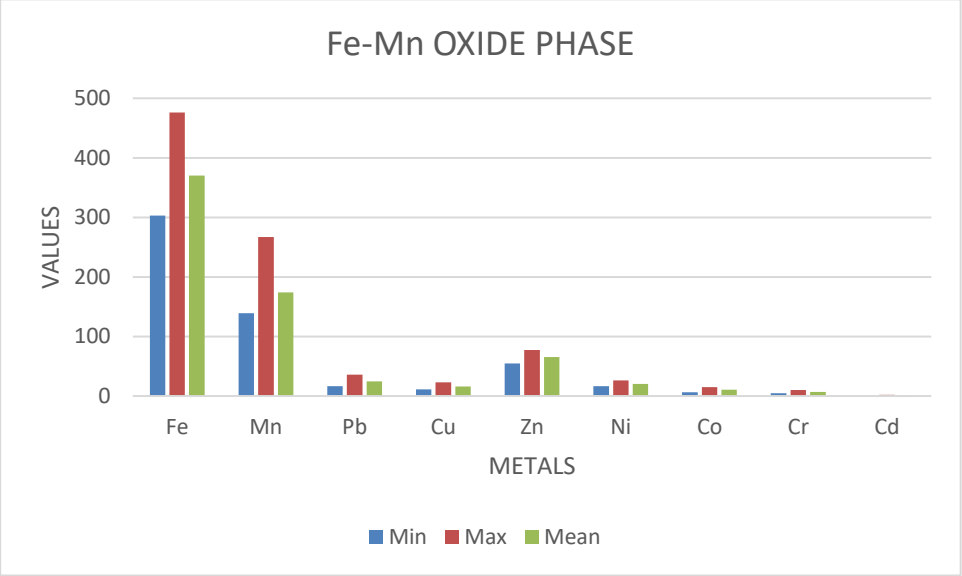

Figure 7. Cluster column chart of the heavy metal concentrations in the Fe–Mn oxide phase (mg/kg). The figure illustrates the comparative distribution of metals across all samples, highlighting strong enrichment and adsorption of trace elements onto Fe–Mn oxide phases within the study area.

4.5 The organic matter–bound phase

The organic matter–bound phase represents metals complexed with humic substances, decomposed organic residues, and microbial materials, and it acts as an important intermediate sink controlling metal retention and delayed release during organic matter decomposition. In tropical soils, this fraction is enhanced by high organic turnover and redox fluctuations, which promote metal–organic complex formation (Kaiser & Kalbitz, 2012; Liu et al., 2022).

From **Table 7a**, Fe shows the highest concentrations (148.854–356.163 mg/kg), indicating strong complexation with organic ligands. Mn (55.772–89.112 mg/kg) also shows appreciable association, reflecting its redox-sensitive behavior influenced by organic matter (Liu et al., 2022). Among trace metals, Cu (14.158–24.486 mg/kg) and Zn (24.128–40.372 mg/kg) are relatively enriched, confirming their strong affinity for organic functional groups. Pb (9.926–16.562 mg/kg) and Cd (0.414–1.221 mg/kg) occur at lower levels but remain environmentally important due to their potential remobilization during organic matter decomposition.

Ni, Co, and Cr show moderate association with organic matter, suggesting partial complexation and mixed control by both organic and mineral phases. The statistical summary in **Table 7b** confirms the dominance order: Fe > Mn > Zn > Cu > Ni ≈ Pb > Co > Cr > Cd, highlighting Fe and Mn as the major contributors to this fraction.

Spatially, higher concentrations in SQ3, SQ4, and SQ15 suggest zones with stronger organic matter influence, while lower values in SQ6 and SQ10 reflect weaker organic binding. **Figure 8** shows a similar pattern, with Fe and Mn dominating, followed by Cu and Zn, while Pb, Cd, Ni, Co, and Cr remain comparatively low.

Overall, this phase indicates that organic matter plays a key role in stabilizing metals—especially Cu, Zn, Fe, and Mn—while also serving as a potential secondary source under decomposition or changing redox conditions (Alloway, 2013; Kaiser & Kalbitz, 2012).

Table 7a: Heavy metals concentrations in the organic matter–bound phase (mg/kg). The table shows the distribution of metals associated with organic matter across all samples, reflecting their affinity for organic complexation and potential release during organic matter decomposition.

Samples	Fe (mg/Kg)	Mn (mg/Kg)	Pb (mg/Kg)	Cu (mg/Kg)	Zn (mg/Kg)	Ni (mg/Kg)	Co (mg/Kg)	Cr (mg/Kg)	Cd (mg/Kg)
SQ 1	182.012	75.224	12.172	20.032	33.213	12.817	6.915	5.503	0.453
SQ 2	181.654	78.127	13.181	20.215	33.158	13.102	6.429	6.232	0.485
SQ 3	335.147	87.225	14.137	22.864	37.685	16.214	8.105	6.954	0.981
SQ 4	341.401	89.112	16.562	23.509	40.021	18.121	9.012	7.051	1.128
SQ 6	164.319	64.435	10.345	15.861	27.183	10.129	4.971	4.672	0.429
SQ7	168.247	64.247	10.631	15.539	28.011	10.216	5.056	4.956	0.433
SQ 8	189.074	81.236	13.123	20.421	33.786	13.014	6.747	6.143	0.472
SQ 10	148.854	55.772	9.926	14.158	24.128	8.997	4.635	4.329	0.414
SQ 11	152.627	57.201	10.011	15.141	25.091	9.089	4.921	4.457	0.425
SQ 12	169.612	65.236	11.162	16.214	25.274	10.176	5.068	4.781	0.446
SQ 13	169.881	64.837	11.134	16.452	25.181	10.089	5.112	8.714	0.451
SQ 14	180.575	76.294	12.634	21.052	32.846	12.763	6.557	5.773	0.472
SQ 15	356.163	87.826	15.663	24.486	40.372	18.522	9.138	7.074	1.221
SQ 16	185.052	75.135	12.246	20.415	33.325	13.012	6.751	6.028	0.482
SQ 17	168.176	65.095	10.773	15.404	28.197	10.332	6.904	6.193	0.462

Table 7b: Statistical summary of the heavy metals in the organic matter–bound phase (mg/kg). The table presents the minimum, maximum, and mean concentrations of metals associated with organic matter, indicating their degree of complexation and relative stability within this geochemical fraction.

Metal	Fe	Mn	Pb	Cu	Zn	Ni	Co	Cr	Cd
Min	148.854	55.772	9.926	14.158	24.128	8.997	4.635	4.329	0.414
Max	356.163	89.112	16.562	24.486	40.372	18.522	9.138	8.714	1.221
Mean	206.186	72.467	12.247	18.784	31.165	12.440	6.421	5.924	0.584

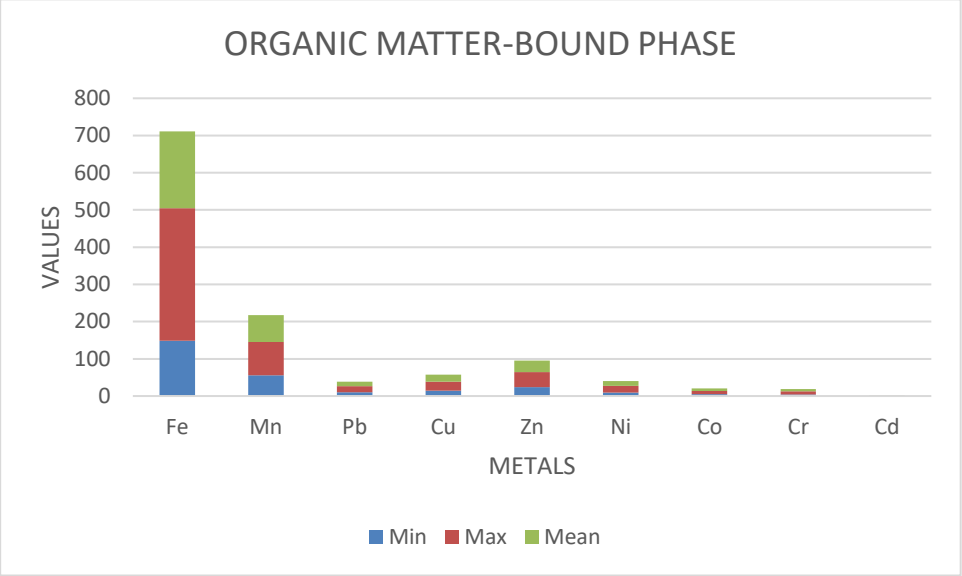

Figure 8. Cluster column chart of the heavy metal concentrations in the organic matter–bound phase (mg/kg). The figure illustrates the distribution of metals across all samples, highlighting their association with organic matter and relative enrichment through complexation with organic ligands.

4.6 The sulfide/strongly bound phase

The sulfide/strongly bound phase represents metals incorporated into sulfide minerals and resistant mineral lattices, and it is generally regarded as the most stable and least mobile fraction in sequential extraction studies. Metals in this fraction are only released under strong oxidizing conditions, making it a long-term geochemical sink for trace elements in soils and sediments (Tessier et al., 1979;).

From **Table 8a**, Fe shows the highest concentrations (184.382–353.506 mg/kg), indicating strong incorporation into resistant and sulfide-related mineral phases. Mn (75.148–150.084 mg/kg) also shows significant association, reflecting co-precipitation under reducing conditions. Among trace metals, Zn (22.101–37.022 mg/kg) and Cu (12.503–22.129 mg/kg) show moderate enrichment, consistent with their known affinity for sulfide mineral formation. Pb (11.016–25.791 mg/kg) is also appreciable, while Cd remains low (0.312–1.147 mg/kg), reflecting its weaker sulfide stability.

Ni, Co, and Cr occur at moderate levels, suggesting partial incorporation into resistant mineral phases. The statistical summary **Table 8b** confirms the dominance order: Fe > Mn > Zn > Cu > Pb > Ni > Co > Cr > Cd, indicating strong geochemical stabilization of Fe and Mn in this fraction.

Spatially, higher values in SQ3, SQ4, and SQ15 suggest localized reducing conditions or sulfide enrichment, while lower values in SQ6 and SQ10 indicate weaker sulfide association. **Figure 9** shows the same pattern, with Fe and Mn dominating across all samples. Overall, this phase represents a stable metal reservoir with low immediate mobility, though it may become a secondary source of metals under oxidative environmental changes (Davidson et al., 1994).

Table 8a: Heavy metal concentrations in the sulfide/strongly bound phase (mg/kg). The table shows metals strongly associated with sulfide minerals and resistant phases, reflecting their low mobility and long-term geochemical stability within the soil matrix.

Samples	Fe (mg/Kg)	Mn (mg/Kg)	Pb (mg/Kg)	Cu (mg/Kg)	Zn (mg/Kg)	Ni (mg/Kg)	Co (mg/Kg)	Cr (mg/Kg)	Cd (mg/Kg)
SQ 1	251.118	105.746	18.723	14.103	31.411	11.652	6.342	5.126	0.343
SQ 2	252.049	108.224	17.916	14.321	30.782	11.761	6.226	5.472	0.345
SQ 3	345.371	147.602	24.432	20.438	35.255	15.004	7.752	6.159	0.798
SQ 4	352.217	147.916	25.543	20.825	36.126	15.243	8.116	6.458	1.128
SQ 6	184.382	83.239	12.621	13.127	26.134	9.827	4.279	4.174	0.312
SQ7	186.641	84.043	12.584	13.312	26.187	10.022	4.853	4.956	0.331
SQ 8	262.248	115.741	19.251	14.329	31.732	12.021	6.349	5.765	0.372
SQ 10	201.508	75.148	11.016	12.503	22.101	8.217	4.251	4.329	0.314
SQ 11	205.421	77.713	11.172	13.008	23.061	8.734	4.584	4.457	0.325
SQ 12	216.142	85.062	11.729	13.543	27.658	10.964	5.866	4.586	0.337
SQ 13	217.618	84.927	11.972	13.729	27.851	11.492	5.982	8.148	0.421
SQ 14	250.354	106.109	18.649	15.021	30.496	12.035	6.264	5.228	0.432
SQ 15	353.506	150.084	25.791	22.129	37.022	15.232	8.335	6.784	1.147
SQ 16	253.127	107.732	18.069	16.011	32.029	12.022	6.016	5.822	0.441
SQ 17	184.783	85.106	11.967	12.938	25.867	10.112	5.241	5.013	0.437

Table 8b: Statistical summary of the heavy metals concentration in the sulfide/strongly bound phase (mg/kg). This table presents the minimum, maximum, and mean concentrations of metals strongly bound within sulfide and resistant mineral phases, indicating their low mobility and high geochemical stability.

Metal	Fe	Mn	Pb	Cu	Zn	Ni	Co	Cr	Cd
Min	184.382	75.148	11.016	12.503	22.101	8.217	4.251	4.174	0.312
Max	353.506	150.084	25.791	22.129	37.022	15.243	8.335	8.148	1.147
Mean	247.766	104.293	16.762	15.289	29.581	11.623	6.030	5.498	0.499

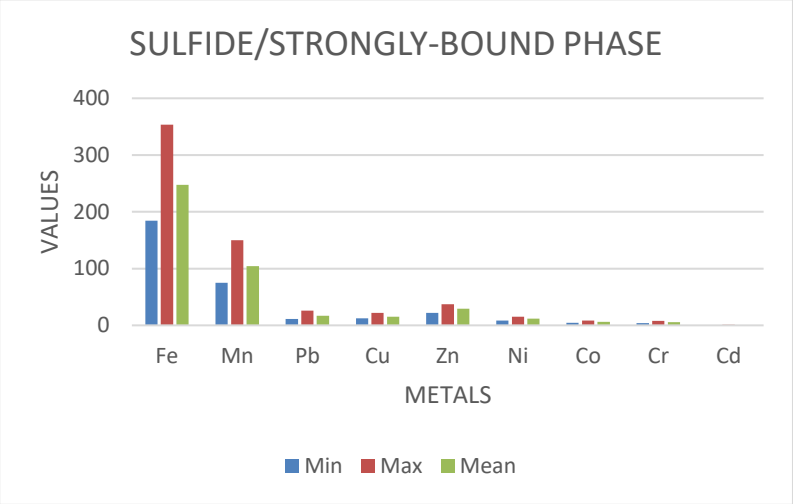

Figure 9. Cluster column chart of the heavy metal concentrations in the sulfide/strongly bound phase (mg/kg). The figure illustrates the distribution of metals strongly bound to sulfide and resistant mineral phases across all samples, highlighting their relative stability and low mobility in the geochemical system.

4.7 The residual phase

The residual phase represents metals strongly incorporated within primary and secondary mineral lattices (e.g., silicates, aluminosilicates, and resistant oxides), and it is widely regarded as the most stable and least mobile fraction in sequential extraction studies. Metals in this fraction are generally considered geochemically inert under normal environmental conditions and are only released through prolonged weathering or complete mineral breakdown (Tessier et al., 1979; Kabata-Pendias, 2011).

From **Table 9a**, Fe exhibits extremely high concentrations (12,532.459–16,416.143 mg/kg), confirming its dominance within primary silicate and ferromagnesian mineral structures. Mn (769.814–946.516 mg/kg) also shows strong lithogenic control, reflecting incorporation into silicate lattices and resistant oxide phases. Among trace metals, Zn (65.905–97.151 mg/kg) and Cu (51.031–62.631 mg/kg) occur at moderate levels, indicating structural substitution within aluminosilicate minerals (Adriano, (2001). Pb (30.574–42.028 mg/kg) and Ni (29.364–43.833 mg/kg) similarly reflect lithogenic inheritance rather than secondary enrichment. Co (13.196–23.146 mg/kg) and Cr (55.704–80.015 mg/kg) are relatively elevated in this phase, consistent with their strong affinity for incorporation into mafic and ultramafic mineral structures. Cd remains very low (0.414–1.302 mg/kg), reflecting its limited structural incorporation and geochemical rarity in resistant mineral phases. The statistical summary **Table 9b** confirms the dominance order: **Fe > Mn > Zn > Cr > Cu > Ni > Co > Pb > Cd**, indicating strong lithogenic control and minimal influence of secondary mobilization processes. The narrow variability across samples further supports a uniform bedrock-derived geochemical signature.

Spatially, higher concentrations in SQ3, SQ4, SQ14, and SQ15 reflect zones enriched in ferromagnesian minerals or more mafic lithological influence, while relatively lower values in SQ6, SQ10, and SQ13 suggest more felsic or weathered lithologies. This spatial pattern is consistent with basement complex terrains where elemental distribution is primarily controlled by parent rock composition rather than anthropogenic inputs.

Figure 10 further confirms this interpretation, showing clear dominance of Fe and Mn across all samples, with other trace metals forming subordinate but stable distributions within the residual matrix. This reinforces the conclusion that most metals are locked within primary mineral structures and are not readily available for environmental mobilization.

Overall, the residual phase represents a long-term geochemical reservoir with negligible immediate environmental risk. However, it serves as a key indicator of bedrock composition and mineralogical control in the Ikole–Itapaji area, consistent with established sequential extraction frameworks in crystalline basement environments (Kabata-Pendias, 2011; Alloway, 2013).

Table 9a: Heavy metal concentrations in the residual phase (mg/kg). The table shows metals strongly locked within primary and secondary mineral lattices, representing the most stable and least mobile geochemical fraction in the soil system.

Samples	Fe (mg/Kg)	Mn (mg/Kg)	Pb (mg/Kg)	Cu (mg/Kg)	Zn **(mg/Kg)**	Ni (mg/Kg)	Co (mg/Kg)	Cr (mg/Kg)	Cd (mg/Kg)
SQ 1	13124.153	851.125	37.231	51.609	86.332	31.861	18.715	66.322	0.597
SQ 2	13231.582	862.197	35.793	52.096	84.809	32.168	19.207	66.188	0.553
SQ 3	16265.625	946.516	40.714	62.631	95.119	42.732	23.061	78.751	1.177
SQ 4	16416.143	941.849	42.028	61.979	97.151	43.833	23.146	80.015	1.185
SQ 6	15693.198	874.034	38.624	56.235	93.009	40.635	21.081	72.231	0.682
SQ7	12758.903	780.623	32.627	53.018	66.745	30.561	13.196	57.592	0.414
SQ 8	14753.727	865.106	36.942	54.723	88.126	34.642	20.731	68.685	1.127
SQ 10	12593.684	789.702	30.574	51.052	65.905	29.364	14.211	55.885	0.534
SQ 11	12682.363	776.937	31.077	51.031	68.016	29.902	13.723	55.759	0.511
SQ 12	14723.794	867.369	38.362	56.387	86.972	34.558	20.148	69.101	0.746
SQ 13	12532.459	769.814	30.984	52.125	68.132	32.092	13.741	55.704	0.642
SQ 14	15562.525	876.614	39.072	58.521	90.165	38.965	22.094	73.672	0.779
SQ 15	15469.538	872.607	40.729	57.985	92.007	39.018	21.628	71.961	1.302
SQ 16	13063.523	856.735	35.071	53.081	84.717	35.109	18.591	67.412	0.698
SQ 17	13274.221	842.699	34.866	52.983	85.458	35.238	18.793	66.923	0.602

Table 9b: Statistical summary of heavy metals in the residual phase (mg/kg). This table presents the minimum, maximum, and mean concentrations of metals retained in the residual fraction, representing the most stable and structurally bound geochemical pool in the soil matrix.

Metal	**Fe**	**Mn**	**Pb**	**Cu**	**Zn**	**Ni**	**Co**	**Cr**	**Cd**
Min	12532.459	769.814	30.574	51.031	65.905	29.364	13.196	55.704	0.414
Max	16416.143	946.516	42.028	62.631	97.151	43.833	23.146	80.015	1.302
Mean	14143.029	851.595	36.313	55.030	83.511	35.379	18.804	67.080	0.770

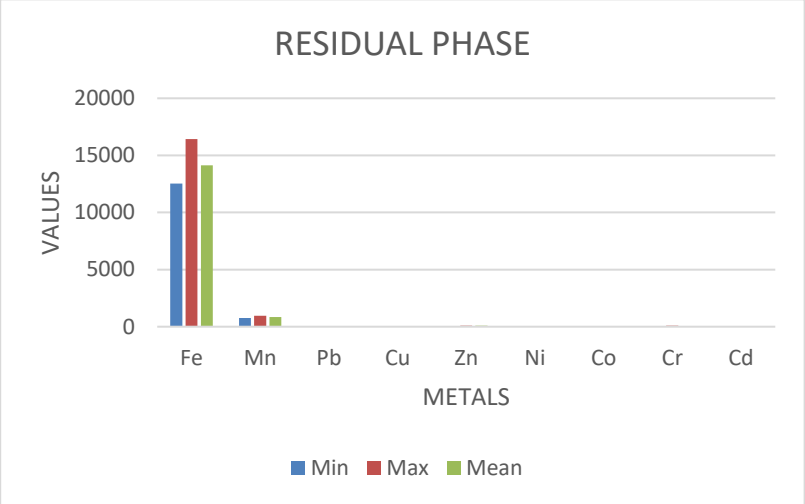

Figure 10. Cluster column chart of the heavy metal concentrations in the residual phase (mg/kg). The figure illustrates the distribution of metals in the residual fraction, highlighting their strong lithogenic control and dominance within primary mineral structures across all samples.

4.8 Geo-accumulation Index (Igeo)

The Geo-accumulation Index (Igeo) values for heavy metals in soils of the Ikole–Itapaji area (SQ1–SQ17) provide a clear assessment of contamination intensity relative to average shale background concentrations. Overall, the results reveal strong variability in metal enrichment across the study area, reflecting both geogenic influences from basement lithologies and localized anthropogenic inputs (Tessier et al., 1979).

Iron (Fe) and manganese (Mn) generally exhibit negative to near-zero Igeo values across most sampling locations, indicating minimal enrichment and a predominantly lithogenic origin. In contrast, trace metals such as Pb, Cu, Zn, Ni, Co, and especially Cd show positive Igeo values in several locations, suggesting varying degrees of contamination and enrichment. Cadmium (Cd) stands out as the most significantly enriched element across all sampling points, with values ranging from moderate to very strong contamination, particularly at SQ3 (3.460), SQ4 (3.627), SQ15 (3.698), and SQ8 (2.918). This indicates a strong anthropogenic influence and/or secondary geochemical concentration processes.

Lead (Pb) also shows moderate enrichment across most sites (generally Igeo > 1), with higher values observed in SQ3, SQ4, and SQ15, suggesting potential inputs from agricultural activities, waste disposal, or lithological sources enriched in sulphide mineralization. Copper (Cu), zinc (Zn), and cobalt (Co) exhibit low to moderate enrichment levels, with spatial clustering of slightly elevated values in SQ3, SQ4, SQ8, SQ14, and SQ15. Nickel (Ni) and chromium (Cr), however, largely remain in the unpolluted to moderately polluted range, indicating limited enrichment and stronger geogenic control (Reimann & de Caritat, 2005) (**Table 10).**

Spatially, **Figure 11** highlights distinct contamination hotspots, particularly around SQ3, SQ4, SQ8, and SQ15, where multiple metals simultaneously show elevated Igeo values. These areas may correspond to zones of intensified human activity or favourable lithological conditions such as migmatite–gneiss transitions that enhance metal retention and accumulation (Reimann & de Caritat, 2005).

The interpretation of heavy metal enrichment in this study aligns with established geochemical principles that emphasize the combined influence of natural background variability and anthropogenic inputs in controlling soil contamination patterns (Reimann & de Caritat, 2005; Förstner & Wittmann, 2012). Such

frameworks are widely used in environmental geochemistry to distinguish between lithogenic and anthropogenic sources of trace metals and to contextualize spatial variations in soil quality.

Overall, the Igeo results demonstrate that while the study area is largely influenced by natural geochemical background levels for some metals, there is clear evidence of significant enrichment—particularly for Cd and Pb—indicating mixed geogenic–anthropogenic controls on soil contamination (Turekian, et al.,1961).

Table 10. Geo-accumulation Index (Igeo) of heavy metals in soils of the Ikole–Itapaji area (SQ1–SQ17), assessing the degree of metal enrichment relative to background concentrations and providing an evaluation of soil contamination intensity across the sampled locations.

Sample	Fe	Mn	Pb	Cu	Zn	Ni	Co	Cr	Cd
SQ1	-2.342	-0.071	1.682	0.610	0.686	-0.391	0.629	-0.686	2.218
SQ2	-2.330	-0.025	1.604	0.640	0.669	-0.360	0.656	-0.672	2.231
SQ3	-2.019	0.197	1.951	0.952	0.879	-0.038	0.957	-0.404	3.460
SQ4	-2.005	0.199	2.041	0.978	0.925	0.063	1.007	-0.368	3.627
SQ6	-2.105	-0.082	1.578	0.592	0.652	-0.295	0.573	-0.634	2.219
SQ7	-2.388	-0.204	1.402	0.546	0.477	-0.513	0.261	-0.863	2.044
SQ8	-2.179	0.002	1.719	0.670	0.741	-0.306	0.737	-0.586	2.918
SQ10	-2.413	-0.231	1.208	0.422	0.334	-0.652	0.089	-0.949	2.075
SQ11	-2.399	-0.234	1.288	0.476	0.395	-0.563	0.207	-0.937	2.089
SQ12	-2.190	-0.094	1.557	0.654	0.598	-0.388	0.591	-0.661	2.356
SQ13	-2.410	-0.219	1.429	0.604	0.465	-0.426	0.362	-0.770	2.361
SQ14	-2.109	-0.009	1.710	0.756	0.703	-0.222	0.739	-0.544	2.563
SQ15	-2.082	0.157	2.026	0.969	0.904	-0.011	0.936	-0.474	3.698
SQ16	-2.347	-0.059	1.596	0.678	0.682	-0.322	0.641	-0.628	2.504
SQ17	-2.337	-0.132	1.376	0.543	0.582	-0.422	0.584	-0.620	2.501

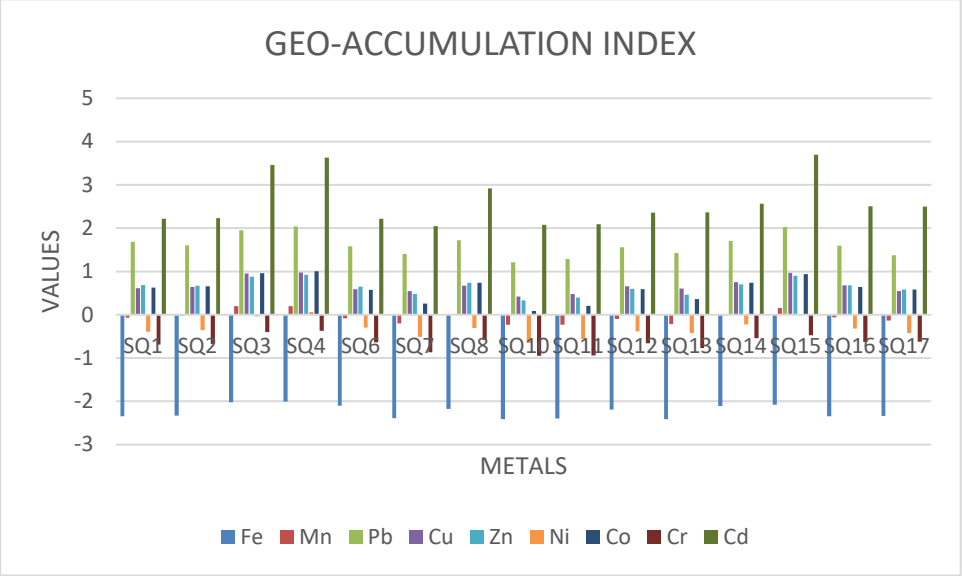

Figure 11. Clustered column chart showing the geo-accumulation index (Igeo) of heavy metals in soils of the study area, illustrating the degree of metal enrichment across sampling locations and highlighting spatial variations in contamination intensity.

4.9 The Enrichment Factor (EF)

The Enrichment Factor (EF) values presented in **Table 11 and Figure 11** provide insight into the sources and degree of heavy metal enrichment within the soils of the Ikole–Itapaji area. Generally, EF values close to 1 indicate a predominantly lithogenic origin, while values greater than 2 suggest anthropogenic influence and metal enrichment (Förstner & Wittmann, 2012; Reimann & de Caritat, 2005).

The results show that Mn, Cu, Zn, Ni, Co, and Cr exhibit relatively low and uniform EF values across most sampling locations, indicating minimal enrichment and suggesting that their concentrations are mainly controlled by the weathering of the underlying basement rocks. The limited spatial variation of these metals further supports their predominantly geogenic origin.

In contrast, Pb and particularly Cd display significantly higher EF values throughout the study area. Cadmium shows the greatest enrichment, indicating substantial accumulation above natural background levels, while Pb exhibits moderate enrichment at several locations. Such enrichment patterns suggest contributions from anthropogenic sources such as agricultural inputs, waste disposal activities, and other localized human activities.

Spatially, the highest enrichment levels occur at SQ4 and SQ15, identifying these locations as major contamination hotspots. Conversely, SQ10 and SQ11 record the lowest enrichment values, reflecting relatively unimpacted conditions. The selective enrichment of Cd and Pb, while most other metals remain near background levels, indicates localized anthropogenic contamination superimposed on a largely natural geochemical environment (Müller, (1969).

Overall, the EF results suggest that the soils of the Ikole–Itapaji area are predominantly influenced by natural geological processes, with notable anthropogenic enrichment of Cd and Pb at specific locations (Tessier et al., 1979; Reimann & de Caritat, 2005).

Table 11. Enrichment Factor (EF) of heavy metals in soils of the Ikole–Itapaji area (SQ1–SQ17), indicating the degree of anthropogenic versus geogenic contribution to metal concentrations and assessing the level of elemental enrichment relative to background reference values.

Sample	Mn	Pb	Cu	Zn	Ni	Co	Cr	Cd
SQ1	0.98	2.61	1.12	1.05	0.86	1.43	0.72	8.91
SQ2	0.95	2.45	1.08	1.02	0.88	1.41	0.71	8.77
SQ3	1.10	3.02	1.36	1.18	0.92	1.66	0.89	14.32
SQ4	1.12	3.18	1.42	1.22	1.01	1.71	0.93	15.41
SQ6	0.99	2.48	1.09	1.07	0.89	1.39	0.70	8.62
SQ7	0.96	2.31	1.04	0.98	0.82	1.18	0.66	7.89
SQ8	1.04	2.72	1.15	1.11	0.91	1.52	0.81	11.23
SQ10	0.92	2.05	0.88	0.74	0.68	0.72	0.55	8.34
SQ11	0.93	2.14	0.91	0.79	0.74	0.81	0.60	8.46
SQ12	1.01	2.46	1.08	1.02	0.86	1.39	0.73	9.21
SQ13	0.98	2.39	1.06	0.97	0.84	1.32	0.74	9.33
SQ14	1.07	2.68	1.21	1.10	0.95	1.55	0.79	10.18
SQ15	1.12	3.14	1.38	1.24	0.99	1.68	0.88	15.77
SQ16	1.00	2.52	1.11	1.06	0.90	1.44	0.73	10.02
SQ17	0.97	2.37	1.07	1.01	0.85	1.36	0.70	9.88

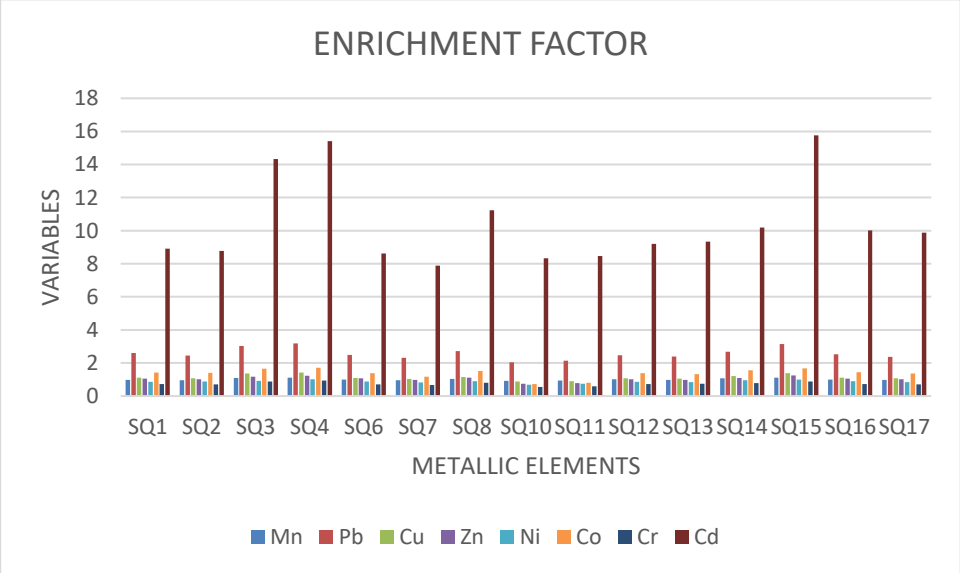

Figure 12. Clustered column chart showing the enrichment factors of heavy metals in soils of the study area, illustrating the degree of metal enrichment across sampling locations and highlighting spatial variations in contamination intensity.

5.0 CONCLUSION

This study evaluated the geochemical distribution, mobility, bioavailability, and contamination status of heavy metals in soils of the Ikole–Itapaji area, Southwestern Nigeria, using sequential extraction procedures, Geo-accumulation Index (Igeo), and Enrichment Factor (EF) analyses. The results reveal that heavy metal occurrence is predominantly controlled by lithological and geochemical processes associated with the underlying Precambrian Basement Complex rocks.

Sequential extraction results indicate that the water-soluble and exchangeable fractions contain relatively low concentrations of all investigated metals, suggesting limited immediate mobility and bioavailability. The carbonate-bound fraction contains moderate metal concentrations, indicating that some metals may become available under acidic environmental conditions. Significant proportions of Fe, Mn, Zn, Pb, and Cu occur within the Fe–Mn oxide and organic matter-bound fractions, demonstrating the important role of adsorption, co-precipitation, and organic complexation in controlling metal retention within the soil system. The sulfide/strongly bound fraction further confirms the stability of most metals under present environmental conditions.

The residual fraction constitutes the dominant reservoir for most investigated metals, particularly Fe, Mn, Zn, Cr, Cu, and Ni. This dominance indicates that the majority of metals are structurally incorporated within primary and secondary mineral lattices and are therefore largely immobile and of lithogenic origin. The predominance of metals in the residual phase suggests that natural weathering of basement rocks represents the principal source of heavy metals in the study area.

Geo-accumulation Index (Igeo) results show that Fe, Mn, Ni, and Cr are generally within unpolluted to moderately polluted categories, reflecting strong geogenic control. However, Cd and Pb display elevated Igeo values at several locations, particularly SQ3, SQ4, SQ8, and SQ15, indicating moderate to strong enrichment and localized contamination. Similarly, Enrichment Factor (EF) analysis demonstrates that Mn, Cu, Zn, Ni, Co, and Cr are largely derived from natural geological sources, whereas Cd and Pb exhibit significant enrichment above background levels, suggesting anthropogenic contributions.

The combined Igeo and EF results identify SQ3, SQ4, and SQ15 as major enrichment hotspots where geogenic processes may be reinforced by localized human activities such as agriculture, waste disposal, and other land-use practices. Nevertheless, the overall contamination level of the study area remains relatively low, with most metals occurring in stable geochemical fractions that pose minimal immediate environmental risk.

Conclusively, the soils of the Ikole–Itapaji area are predominantly influenced by natural geological processes, with most heavy metals strongly retained within stable mineral phases. However, the elevated enrichment of Cd and Pb at specific locations highlights the need for periodic environmental monitoring and sustainable land-management practices to prevent future accumulation and potential ecological impacts. The study provides valuable baseline geochemical information for environmental assessment, land-use planning, and mineral exploration within the Basement Complex terrain of Southwestern Nigeria.

5.1 Recommendations

Based on the findings of this study, the following recommendations are proposed:

1. **Periodic Environmental Monitoring:** Regular monitoring of heavy metal concentrations should be conducted in the Ikole–Itapaji area, particularly at sampling locations SQ3, SQ4, SQ8, and SQ15, where elevated Cd and Pb enrichment was observed. This will help detect any future increase in contamination levels and assess long-term environmental trends.
2. **Control of Anthropogenic Inputs:** Efforts should be made to regulate agricultural practices, waste disposal activities, and other human-related activities that may contribute to Cd and

Pb accumulation in soils. The use of fertilizers, pesticides, and agrochemicals containing trace metals should be carefully monitored.

3. **Detailed Source Identification Studies:** Further investigations involving isotopic analysis, mineralogical characterization, and multivariate statistical techniques are recommended to distinguish more clearly between lithogenic and anthropogenic sources of Cd and Pb enrichment.
4. **Integration with Groundwater and Plant Studies:** Future studies should assess heavy metal concentrations in groundwater, surface water, and crops within the study area to evaluate potential transfer pathways and associated ecological or human health risks.
5. **Geochemical and Mineral Exploration Applications:** The observed concentration of metals in the Fe–Mn oxide, organic matter-bound, and residual fractions suggests that sequential extraction studies should be integrated with geological, geophysical, and geochemical exploration programs to improve understanding of mineralization processes within the Basement Complex terrain.
6. **Land-Use Planning and Environmental Management:**

   Environmental impact assessments should be incorporated into future land-use and agricultural development programs to minimize potential heavy metal accumulation and maintain soil quality.

5.2 Limitations of the Study

Despite providing valuable information on heavy metal distribution and speciation within the Ikole–Itapaji area, this study has some limitations:

1. **Limited Spatial Coverage:** The study was based on seventeen soil samples, which may not fully capture all local geochemical variations across the entire study area.
2. **Seasonal Variability Not Considered:** Sampling was conducted during a single period; therefore, seasonal effects on metal mobility, redistribution, and bioavailability were not evaluated.
3. **Restricted Number of Metals Analyzed:** Only selected heavy metals (Fe, Mn, Pb, Cu, Zn, Ni, Co, Cr, and Cd) were investigated. Other potentially important trace elements and rare metals were not included.
4. **Operational Nature of Sequential Extraction:** The sequential extraction procedure provides operationally defined fractions rather than exact mineralogical phases. Consequently, some overlap among extraction fractions may occur.
5. **Lack of Mineralogical Verification:** Detailed mineralogical analyses such as X-ray diffraction (XRD), scanning electron microscopy (SEM), or electron microprobe studies were not conducted to directly confirm the host mineral phases of the metals.
6. **No Human Health Risk Assessment:** Although contamination indices were evaluated, the study did not quantify ecological or human health risks associated with heavy metal exposure.
7. **Absence of Supporting Hydrogeochemical Data:** Groundwater, surface water, and vegetation samples were not analyzed; therefore, the potential migration of metals through the broader environmental system could not be fully assessed.

Overall, these limitations do not diminish the reliability of the findings but highlight areas where future investigations can expand and strengthen the understanding of heavy metal behavior, contamination sources, and environmental implications in the Ikole–Itapaji Basement Complex terrain.

Availability of Data and Materials

The datasets used and analyzed during this study are available from the corresponding author upon reasonable request.

Disclaimer (Artificial Intelligence)

During the preparation of this work, the authors used ChatGPT (GPT-5-mini) to assist with language editing and content organization. After using this tool, the authors reviewed, revised, and verified all content to ensure accuracy, originality, and authenticity, and take full responsibility for the content of the published article.

Competing Interests

The authors have declared that no competing interests exist.

Authors' Contributions

Adeleke Ojo contributed to the conceptualization and design of the study, field sampling, laboratory analysis, data interpretation, and preparation of the initial manuscript draft. **Olusola Amos Olaolorun** was involved in the supervision of the research work, methodological review, interpretation of geochemical results, and critical revision of the manuscript for important intellectual content. **Segun Ajayi AKINYEMI** contributed to data processing, statistical and geochemical analysis, literature review, and editing of the final manuscript. All authors read and approved the final version of the manuscript.

REFERENCES

1. Abule, E. C., & Ekpete, O. A. (2025). Geochemical speciation and environmental implications of heavy metal mobility. https://doi.org/10.63561/fnas-jsi.v6i3.955
2. Adetunla, F. R., Ayodele, O. S., Asowata, I. T., & Olususi, J. (2025). Integrated geological, aeromagnetic and remote sensing datasets in litho-structural mapping of basement rocks in southwestern Nigeria. *Asian Journal of Geological Research, 8*(3), 523–553. https://doi.org/10.9734/ajoger/2025/v8i3213
3. Adriano, D. C. (2001). *Trace Elements in Terrestrial Environments: Biogeochemistry, Bioavailability, and Risks of Metals*. Springer, New York. https://link.springer.com/book/10.1007/978-0-387-21510-5
4. Alloway, B. J. (2013). *Heavy Metals in Soils: Trace Metals and Metalloids in Soils and Their Bioavailability* (3rd ed.). Springer. https://doi.org/10.1007/978-94-007-4470-7
5. Birth, G. (2003). A scheme for assessing human impacts on coastal aquatic environments using sediments. https://doi.org/10.1007/978-3-662-05950-8_7
6. Bouazizi, N., Baraud, F., Lemoine, M., & Leleyter, L. (2023). Shortened sequential extraction procedure: An effective and time-saving determination of trace metals in sediments. *Soil and Sediment Contamination*. https://doi.org/10.1080/15320383.2023.2293879
7. Çelebi, E. E. (2024). Determination of metal fractions and rare earth anomalies using modified sequential extraction. *Environmental Earth Sciences, 83*, 93. https://doi.org/10.1007/s12665-023-11409-w
8. Davidson, C. M., Duncan, A. L., Littlejohn, D., Ure, A. M., & Garden, L. M. (1998). A critical evaluation of the three-stage BCR sequential extraction procedure to assess the potential mobility and toxicity of heavy metals in industrially contaminated land. *Analytica Chimica Acta, 363*(1–2), 45–55. https://doi.org/10.1016/S0003-2670(98)00057-9
9. De Matteis, C., Mantovani, L., Tribaudino, M., et al. (2023). Sequential extraction procedure of municipal solid waste incineration bottom ash targeting grain size and amorphous fraction. *Frontiers in Environmental Science, 11*, 1254205. https://doi.org/10.3389/fenvs.2023.1254205

10. Delina, R. E. G. (2024). Partitioning and mobility of chromium using sequential extraction. *Environmental Science & Technology*. https://doi.org/10.1021/acs.est.3c10774

11. Doi, T., Hamasaki, S., Yamamoto, H., et al. (2023). Dynamic sequential extraction procedure for extracting mercury from soil samples. *Analytical Sciences, 39*(5), 739–748. https://doi.org/10.1007/s44211-023-00313-9

12. Filgueiras, A. V., Lavilla, I., & Bendicho, C. (2002). Chemical sequential extraction for metal partitioning in environmental solid samples. *Journal of Environmental Monitoring, 4*, 823–857. https://doi.org/10.1039/B207574C

13. Firmino, F. H. T., et al. (2025). Efficiency of sequential extraction schemes in partitioning toxic elements. *European Journal of Soil Science*. https://doi.org/10.1111/ejss.70090

14. Förstner, U., & Wittmann, G. T. W. (2012). *Metal Pollution in the Aquatic Environment*. Springer. https://doi.org/10.1007/978-3-642-69385-4

15. Hakanson, L. (1980). An ecological risk index for aquatic pollution control: A sedimentological approach. *Water Research, 14*(8), 975–1001. https://doi.org/10.1016/0043-1354(80)90143-8

16. Ibrahim, R., et al. (2024). Sequential extraction of heavy metals in soils. https://doi.org/10.33003/fjs-2024-0803-2451

17. Kabata-Pendias, A. (2011). *Trace Elements in Soils and Plants* (4th ed.). CRC Press. https://doi.org/10.1201/b10158

18. Kaiser, K., & Kalbitz, K. (2012). Cycling downwards – dissolved organic matter in soils. *Soil Biology and Biochemistry, 52*, 29–32. https://doi.org/10.1016/j.soilbio.2012.04.002

19. Liu, J., et al. (2022). Speciation of heavy metals in soils and their immobilization at micro-scale interfaces among soil components. *Science of the Total Environment, 825*, 153862. https://doi.org/10.1016/j.scitotenv.2022.153862

20. Müller, G. (1969). Index of geoaccumulation in sediments of the Rhine River. *GeoJournal, 2*(3), 108–118. https://www.semanticscholar.org/paper/INDEX-OF-GEOACCUMULATION-IN-SEDIMENTS-OF-THE-RHINE-Muller/03688e2c0b4cabea9023db05e6b9a33281f0ea06

21. Nigerian Geological Survey Agency (NGSA). (2006). *Geophysical Mapping of Nigeria: Airborne Radiometric and Magnetic Survey Data, 2006*. Available at: https://ngsa.gov.ng

22. Ogah, A. J., & Abubakar, F. (2024). Solid mineral potential evaluation using integrated aeromagnetic and aeroradiometric datasets. *Scientific Reports, 14*, 1637. https://doi.org/10.1038/s41598-024-52270-6

23. Ojo, O. F., Osazuwa, B. I., Chiemeke, C. C., Osumeje, O. J., Oyedele, A. A., Adagunodo, T. A., Oyeyemi, K. D., & Ejiga, E. G. (2024). Classification of the basement complex using aeromagnetic and remote sensing data analyses: Case study of Ekiti State, southwestern Nigeria. *Earth Sciences Malaysia, 8*(2), 158–162. https://doi.org/10.26480/esmy.02.2024.158.162

24. Oyinloye, A. O. (2011). Geology and geotectonic setting of the basement complex rocks in Southwestern Nigeria: Implications on provenance and evolution. https://doi.org/10.5772/26990

25. Rahaman, M. A. (1988). Recent Advances in the Study of the Basement Complex of Nigeria. In *Precambrian Geology of Nigeria* (pp. 11–41). Geological Survey of Nigeria, Kaduna.

https://www.scirp.org/reference/referencespapers?referenceid=1712445

26. Reimann, C., & de Caritat, P. (2005). Distinguishing between natural and anthropogenic sources for elements in the environment. *Science of the Total Environment, 337*, 91–107. https://doi.org/10.1016/j.scitotenv.2004.06.011
27. Reimann, C., & de Caritat, P. (2012). *Chemical Elements in the Environment: Factsheets for the Geochemist and Environmental Scientist*. Springer. https://doi.org/10.1007/978-3-642-72016-1
28. Salako, K. A., Adetona, A. A., Rafiu, A. A., Augie, A. I., Jimoh, M. O., Alkali, A., Muriana, R. A., & Lawrence, J. O. (2024). Integrated geophysical investigation for gold mineralization potential over the southern parts of Kebbi State, northwestern Nigeria. *Heliyon*, *10*(14), e34093. https://doi.org/10.1016/j.heliyon.2024.e34093
29. Souza, J. P. R., Garnier, J., Quintarelli, J. M., et al. (2024). Adapted sequential extraction protocol for mercury speciation in mining environments. *Toxics*, *12*(5), 326. https://doi.org/10.3390/toxics12050326
30. Tessier, A., Campbell, P. G. C., & Bisson, M. (1979). Sequential extraction procedure for the speciation of particulate trace metals. *Analytical Chemistry, 51*, 844–851. https://doi.org/10.1021/ac50043a017
31. Turekian, K. K., & Wedepohl, K. H. (1961). Distribution of the elements in some major units of the Earth's crust. *Geological Society of America Bulletin*, *72*(2), 175–192. https://doi.org/10.1130/0016-7606(1961)72[175:DOTEIS]2.0.CO;2
32. Wei, B., & Yang, L. (2010). A review of heavy metal contaminations in urban soils, urban road dusts and agricultural soils from China. *Microchemical Journal*, *94*(2), 99–107. https://doi.org/10.1016/j.microc.2009.09.014